TRIBHUVAN UNIVERSITY

INSTITUTE OF ENGINEERING

PULCHOWK CAMPUS

THESIS NO. PUL079MSGtE004

Settlement Analysis of Labim Mall Using Plaxis-3D

by

Anurag Poudel

A THESIS

SUBMITTED TO THE DEPARTMENT OF CIVIL ENGINEERING

IN PARTIAL FULFILLMENT OF THE REQUIREMENTS FOR THE

DEGREE OF MASTERS OF SCIENCE IN

GEOTECHNICAL ENGINEERING

DEPARTMENT OF CIVIL ENGINEERING

LALITPUR, NEPAL

APRIL, 2026

COPYRIGHT

The author has agreed that the library, Department of Civil Engineering, Pulchowk Campus, Institute of Engineering, may make this thesis freely available for inspection.

Moreover, the author has agreed that permission for extensive copying of this thesis for scholarly purpose may be granted by the professor(s) who supervised the work recorded herein or, in their absence, by the Head of the Department wherein the thesis was done. It is understood that the recognition will be given to the author of this thesis and to the Department of Civil Engineering, Pulchowk Campus, Institute of Engineering in any use of the material of this thesis. Copying or publication or the other use of this thesis for financial gain without approval of the Department of Civil Engineering, Pulchowk Campus, Institute of Engineering and author's written permission is prohibited.

Request for permission to copy or to make any other use of the material in this thesis in whole or in part should be addressed to:

.....

Head

Department of Civil Engineering

Pulchowk Campus, Institute of Engineering

Lalitpur, Nepal

TRIBHUVAN UNIVERSITY

INSTITUTE OF ENGINEERING

PULCHOWK CAMPUS

DEPARTMENT OF CIVIL ENGINEERING

The thesis titled **"Settlement Analysis of Labim Mall Using Plaxis-3D"** prepared and submitted by Mr. Anurag Poudel (PUL079MSGtE004) in partial fulfilment of the requirements for the degree of Master of Science (M. Sc.) in Geotechnical Engineering has been examined by us and is accepted for the award of M. Sc. in Geotechnical Engineering by Tribhuvan University.

The undersigned certify that they have read, and recommended to the Institute of Engineering for acceptance, a thesis entitled **"Settlement Analysis of Labim Mall Using Plaxis-3D"** submitted by Mr. Anurag Poudel (PUL079MSGtE004) in partial fulfillment of the requirements for the degree of Master of Science in Geotechnical Engineering.

.....

Supervisor:

Prof. Dr. Indra Prasad Acharya

Department of Civil Engineering

Pulchowk Campus, Lalitpur, Nepal

.....

External Examiner:

Er. Prabhat Kumar Jha

Department of Roads

Ministry of Physical Infrastructure and Transport

Government of Nepal

.....

Program Coordinator:

Dr. Bhim Kumar Dahal

M. Sc. in Geotechnical Engineering

Department of Civil Engineering

Pulchowk Campus, Lalitpur, Nepal

Date: April, 2026

DECLARATION

I hereby declare that this study titled "**Settlement Analysis of Labim Mall Using Plaxis-3D**" is based on my original research work. Related works on the topic by other researchers have been duly acknowledged. I owe all the liabilities relating to the accuracy and authenticity of the data and any other information included hereunder.

……..

Anurag Poudel

PUL079MSGtE004

MSc in Geotechnical Engineering

Date: April, 2026

ACKNOWLEDGMENT

It gives me immense pleasure to express my sincere gratitude to all the individuals and institutions who directly or indirectly contributed in the preparation of this thesis report. Without the help and support from these distinguished figures and institutions, this study would not have been possible.

First and foremost, I would like to express my cordial thanks and special gratitude to my supervisor, **Dr. Indra Prasad Acharya** for his guidance and valuable suggestions, comments, and encouragements from the beginning till the completion of this report. And towards our program coordinator **Dr. Bhim Kumar Dahal** for managing the environment for the completion of the report.

Similarly, I extend my gratitude towards all teachers for the technical and administrative help for the research who made my stay at Pulchowk Campus homely and memorable.

My highest recognition and deepest praise to my family who has always supported my dreams and has inspired me to study and conduct the research coupled with my level of knowledge. I owe all my success to them.

ABSTRACT

A detailed settlement analysis of Labim Mall, a major commercial complex located in Pulchowk, Lalitpur, underlain by soft and highly compressible lacustrine soils typical of the Kathmandu Valley is presented in this study. Five boreholes with 30 m depth were evaluated to characterize the soil profile, consisting predominantly of medium-stiff grey silt overlying stiff organic clay with a shallow groundwater table. Settlement was assessed using both analytical methods based on Terzaghi's one-dimensional consolidation theory and advanced numerical modelling using PLAXIS 3D. The analytical approach, incorporating layered soil behavior and consolidation parameters derived from laboratory testing, estimated a primary consolidation settlement of 179.30 mm. And, by empirical analysis using Janbu method, estimates settlement of 172.329 mm. Numerical modelling in PLAXIS 3D, which incorporated three-dimensional staged construction, and raft foundation behavior, predicted an average settlement of 155.94 mm across all boreholes. Both approaches indicate that the building has reached the end of primary consolidation, with approximately 98% consolidation achieved, suggesting that further deformations will be governed mainly by secondary compression. Differential settlement between construction phases was found to be minimal, indicating negligible interaction effects due to sequential block construction.

The comparison of analytical, numerical and empirical results demonstrates good agreement, validating the use of PLAXIS 3D for settlement prediction in complex Kathmandu Valley soils. The findings highlight the importance of rigorous geotechnical characterization and 3D numerical modelling for the performance assessment of large commercial structures resting on soft compressible soil.

Keywords: - Settlement, Primary Consolidation, Plaxis-3D

TABLE OF CONTENT

LIST OF FIGURES

LIST OF TABLES

ABBREVATION AND SYMBOLS

σ	Stress
BH	Borehole
C_c	Compression Index
C_v	Coefficient of Consolidation
DInSAR	Differential Interferometric Synthetic Aperture Radar
e	Void Ratio
Δe	Change in Void Ratio
e_o	Initial Void Ratio
ETABS	Extended Three-Dimensional Analysis of Building Systems
FEM	Finite Element Method
G	Specific Gravity
LL	Liquid Limit
m_v	Coefficient of Volume Change
SPT	Standard Penetration Test
T_v	Time Factor
u_o	Initial pore pressure
U	Average Degree of Consolidation
σ_0	Initial Stress
Υ	Bulk unit weight
Υ_d	Dry unit weight

1 INTRODUCTION

1.1 General

Settlement analysis is one of fundamental aspects of geotechnical engineering, focusing on the downward movement of structures due to the compression of the underlying soil particles. This phenomenon is particularly critical for large commercial structures like malls, where uneven or excessive settlement can lead to significant structural damage, operational disruptions, and safety hazards. The complexity of soil-structure interaction requires advanced analytical tools to predict and manage settlement effectively.

The settlement behavior of large structures such as malls is influenced by a variety of factors such as soil properties, loading conditions, construction methods, and environmental conditions. Inadequate understanding and prediction of these factors can result in differential settlement, which poses significant risks to the integrity and safety of the structure. Traditional methods of settlement analysis may not adequately capture the complex interactions between the soil and the structure, leading to inaccurate predictions and potential failures.

Labim Mall is one of the most prominent and active commercial centers in Lalitpur, attracting many visitors daily. Ensuring the structural integrity of Labim Mall is paramount for the safety and well-being of these visitors. The mall is constructed on soft dark grey to grey silt of medium stiff to stiff of low plasticity upto 16m depth then dark grey stiff organic clay of high plasticity upto 30m, which poses significant challenges regarding soil consolidation and settlement. The consolidation of soil and the resulting settlement can have critical implications for the building's stability.

Given the importance of maintaining the structural safety of Labim Mall, this study focuses on analyzing the settlement of the mall. The research aims to provide a comprehensive understanding of the settlement process and its impact on the structure. By utilizing advanced numerical modeling techniques such as PLAXIS-3D, the study will offer valuable insights into the settlement patterns and propose recommendations to mitigate potential risks. This analysis is essential not only for the current safety of the mall but also for its future sustainability as a key commercial hub in Lalitpur.

(Source: - *Google Map)*

Figure 1.1:- Location of Labim Mall

PLAXIS-3D is a finite element software specifically designed for geotechnical applications for simulating and analyzing soil behavior and its interaction with structures. By utilizing PLAXIS-3D, complex soil conditions and structural loads can be modelled and predict settlement patterns accurately, allowing for more informed design and construction practices.

1.2 Objective of Study

This study aims to leverage the advanced capabilities of PLAXIS-3D to perform a detailed settlement analysis of Labim mall. The study seeks to know settlement behavior of the structure. The outcomes of this research will offer valuable insights into the factors affecting settlement and provide practical recommendations for mitigating settlement-related issues in large commercial buildings.

The primary objectives of this thesis are:

- To analyze the settlement behavior of a selected mall using PLAXIS-3D.
- To analyze the differential settlement.
- To compare the settlement of numerical modelling, analytical method and empirical method.

1.3 Scope

The present study focuses on settlement analysis of Labim Mall, a large-scale commercial complex in Pulchowk, Lalitpur, using PLAXIS 3D finite element software. The work builds upon prior geotechnical research on Kathmandu Valley soils and aims to address the limitations of two-dimensional and purely empirical approaches.

The scope of the study is defined as follows:

- To evaluate total and differential settlement under loading conditions.
- Simulation is performed using PLAXIS 3D, incorporating actual stratigraphy, groundwater levels, and staged construction (excavation + loading).
- The numerical results are validated through analytical, empirical, and literature-based benchmarks from prior Kathmandu Valley studies.

1.4 Structure of Thesis

The study is organized into six chapters and three appendixes to explain the details of background, objective, previous related research, analysis done and the main outcomes of this research.

1 INTRODUCTION gives a brief introduction to this study. This section presents the problem statement followed by the research objective and scope.

2 LITERATURE REVIEW presents the literature review of soil condition of Kathmandu Valley and its behavior with its settlement characteristics.

3 SOIL AND BUILDING PROPERTIES gives site specific information on soil condition and building layout (superstructure, foundation and construction)

4 METHOD OF ANALYSIS gives a detailed information of overall methodology used to meet the objectives of this study. It includes, data acquisition and modelling approach conducted in this study.

5 RESULT AND DISCUSSION presents the result obtained from the analysis in systematic and meaningful manner. This chapter helps to draw conclusions from the study and analysis carried out.

6 CONCLUSION AND RECOMMENDATION this chapter helps to draw conclusions and further recommendation for future work with its limitation.

Appendix - A BOREHOLE LOG presents the detailed borehole logs of the study area, including soil stratification, Standard Penetration Test (SPT) values, groundwater conditions, and sample descriptions.

Appendix - B LOAD CALCULATION includes the structural load calculations obtained from ETABS analysis, which are used as input for settlement analysis. It provides detailed breakdown of dead loads, live loads, and load combinations transferred to the foundation**.**

Appendix - C COEFFICIENT OF CONSOLIDATION presents the calculation of the coefficient of consolidation (C_v) and the degree of consolidation of the underlying soil layers and settlement according to the degree of consolidation.

2 LITERATURE REVIEW

2.1 General

The Kathmandu Valley's soil is derived from Paleo-Kathmandu Lake and river deposits. According to *Paudel and Sakai (2008)*, it consists of gravely alluvial fans in the south and soft clay and silt (especially Kalimati Clay) in the centre. The following layers: Tarebhir, Lukundol, Itaiti, Kalimati, Sunakothi and Terrace Gravels, record the lake to river plain transitional processes of the valley. The result is weak compressible soil which explains the low bearing capacity and susceptibility to earthquake.

The soil of the Kathmandu Valley is mainly silt-clay, which is characterized by low bearing capacity and soft to medium soft soils. The soil test results over 51 points along Kathmandu, Lalitpur, and Bhaktapur mentioned by *Neeru K. C. and Khet Raj Dahal (2020),* have shown that the bearing capacity varies from 56 to about 163 kN/m^2, whereas the SPT N-values are from 4 to 8, signifying weak soils with wide variation in depth of water table (0.5 m to 16.5 m).

According to *Bhattarai et al. (2017)*, the Kathmandu Valley is sinking due to groundwater over-extraction and its soft, unconsolidated soils of clay, silt, and sand. Using satellite DInSAR data (2007–2010), the study found subsidence up to 17 cm in central urban areas like Kathmandu, Lalitpur, and Thimi, making soil subsidence a growing threat to the valley's infrastructure and stability.

Long-term soil deformation, especially creep and secondary consolidation in soft soils, can significantly affect the performance and safety of reinforced concrete (RC) structures. Using a finite-element soil–structure interaction (SSI) model based on the Soft Soil Creep Model (SSCM), the authors demonstrate that settlements at foundations evolve over years, influencing bending moments, differential settlement, and structural stresses. The results highlight that soil compressibility, heterogeneity, and nonlinear time-dependent behavior must be considered in design, as assuming rigid supports can underestimate long-term structural demands *(Bezih et al., 2020).*

The Upper Tamakoshi Hydropower Dam in Nepal settled about 19 cm uniformly during the 2015 Gorkha earthquake, mainly due to compaction of its >100 m thick sediment foundation. Analytical methods using SPT data estimated 6–24 cm of settlement which is consistent with field observations. The study concluded that stronger shaking (PGA > 0.24 g) could have caused 2–2.5 times greater settlement,

emphasizing the need for robust seismic design on soft deposits *(Tiwari, Ajmera & Timbadia, 2019)*.

The total settlements in the building with mat foundation is higher when compared with the building with isolated footings, but the maximum angular distortion is similar. In mat foundation there was less differential settlement but was more in isolated footing *(Quintero et al. 2024)*.

Settlement interaction is influenced by the stiffness and depth of the foundations. For stiff, deep foundation systems, interactions are minor. If one or more buildings are supported on shorter or less stiff foundations, interaction effects become significant. (*Poulos, H. G. 2023).*

A six-story building showed uneven settlement up to 121 mm (estimated 144 mm total), on Kathmandu's soft organic clay (Kalomato), which has low strength and high compressibility, exceeding standard limits but without structural damage *(Handali, S., & Maharjan, S. 2020).*

The settlement of a ten-story building using the Mohr-Coulomb Model (MCM) and the Hardening Soil Model (HSM) in PLAXIS 2D. Results showed that MCM overestimated settlement by 50–65% compared to HSM, though both remained within the allowable limit of 100 mm. The authors concluded that HSM provides more accurate and realistic predictions for multi-story building settlements on variable soil conditions *(Bhutto et al. 2020)*.

Al-Taie et al. (2016) confirm that finite element modeling (PLAXIS 2D) offers more realistic settlement predictions than classical theoretical methods, particularly for soft or heterogeneous soils. Field and laboratory tests in Mosul, Baghdad, and Basrah, representing different soil profiles, to evaluate immediate and consolidation settlements under various loads. Results showed that PLAXIS predicted higher settlements than mathematical methods, emphasizing the influence of soil model choice (Hardening Soil vs. Mohr–Coulomb).

The settlement in concrete-walled buildings on mat foundations, showing that soil–structure interaction and construction sequencing greatly affect performance. Buildings on landfill zones settled more, and partial construction caused distortions. Including SSI and staged construction in design proved essential for accurate settlement prediction and structural safety *(Patrício, J. D et al. 2024).*

Tewatia (2012) proposes a method to assess soil settlement using the rate of settlement, distinguishing primary (linear) and secondary (semi-log)

consolidation trends. This approach helps quickly identify consolidation stages and estimate soil behavior without knowing past loading history.

Secondary compression occurs after primary consolidation and is significant in soils with high organic content. The accelerated incremental load consolidation testing process can be used to calculate the coefficient of secondary compression *(Raheena, M., & Robinson, R. G. 2020)*.

The beginning of secondary compression in soils depends on the load increment ratio, with organic soils showing earlier onset compared to inorganic soils *(Robinson, R. G. 2003).*

2.2 Settlement

Settlement is a key geotechnical parameter influencing the serviceability and long-term stability of buildings, particularly in regions underlain by soft and compressible deposits like the Kathmandu Valley. Total and differential settlements govern the degree of deformation that occurs in soil due to the applied structural load, ultimately affecting the safety and functionality of structures.

According to *Terzaghi and Peck (1967)*, settlement represents the downward vertical movement of the ground surface caused by changes in stress distribution beneath the foundation. It can be categorized into immediate (elastic), primary consolidation, and secondary (creep) components.

In the context of the Kathmandu Valley, where fine-grained lacustrine deposits dominate, primary consolidation settlement is the most significant contributor due to low permeability and high compressibility of silty clay layers.

2.2.1 Total Settlement

Total settlement (S_t) is defined as the sum of all vertical deformations that occur under a loaded foundation system, expressed as:

$$S_t = S_i + S_c + S_s \quad \text{Eq. 2.1}$$

Where,

S_i = immediate settlement

S_c= primary consolidation settlement

S_s = secondary compression (creep) settlement

According to *Bowles (1996) and Das (2016)*, total settlement depends on soil stiffness, stress level, layer thickness, and drainage conditions. For medium-rise

buildings on clayey soils, acceptable total settlements typically range between 40–65 mm, while values exceeding 75 mm may cause noticeable structural distress.

2.2.2 Differential Settlement

While total settlement represents overall vertical displacement, differential settlement (ΔS) measures the variation in settlement between two points along the foundation. It is a critical factor in determining whether the structure will experience distortion or tilting, defined as:

$$\Delta S = | S_{max} - S_{min} | \quad \text{Eq. 2.2}$$

and

$$\beta = \Delta S / L \quad \text{Eq. 2.3}$$

Where,

β denotes angular distortion and

L the distance between reference points.

According to *Poulos and Davis (2011)*, excessive differential settlement, rather than large total settlement is the main cause of structural cracking and damage. IS 1904-2021 suggest that angular distortion should generally not exceed for raft foundation in plastic clay is 1/500 for RC structure and 1/300 for multi storeyed RC or steel framed structure.

2.3 Stages of Settlement

Settlement of foundations is a time-dependent process that occurs in several distinct stages, governed by the interaction between soil type, load intensity, drainage conditions, and time. In cohesive soils such as those of the Kathmandu Valley, settlement does not occur instantaneously but progresses through three major phases — immediate (elastic), primary consolidation, and secondary (creep) settlement.

Each stage represents a specific physical mechanism of soil deformation. The accurate assessment of these stages is vital for understanding both short-term and long-term foundation behavior, particularly in soft alluvial and lacustrine deposits where delayed consolidation dominates total deformation.

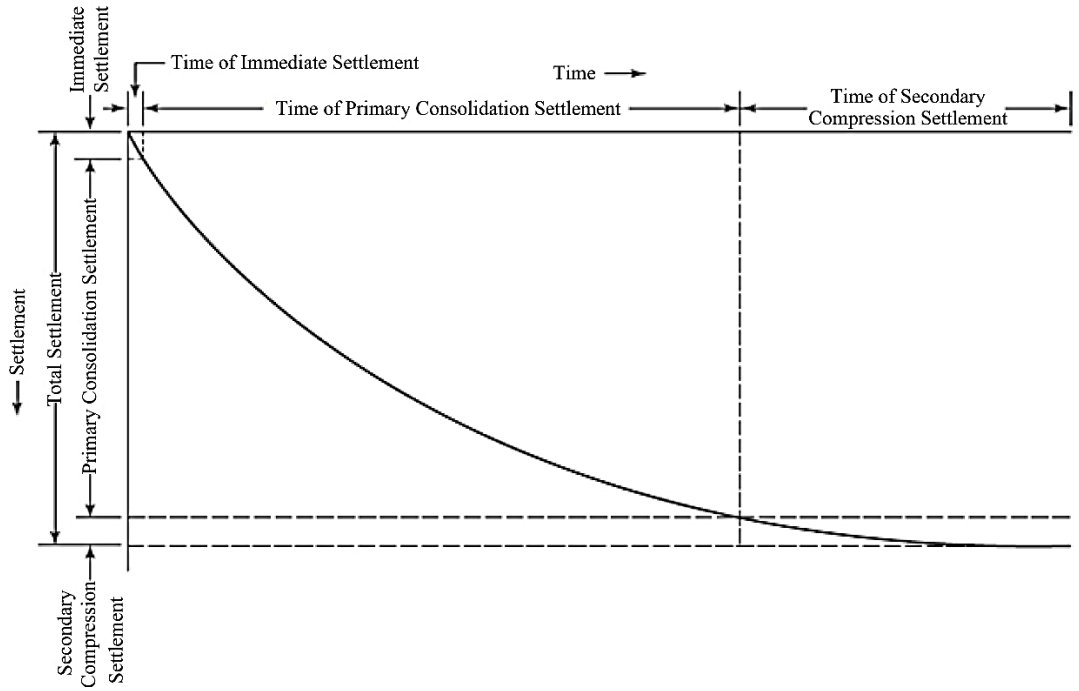

(Source: *Al-Taie, E., Al-Ansari, N., & Knutsson, S. (2016)*)

Figure 2.1 :- Time Settlement Relation

2.3.1 Intermediate Settlement

The first stage of settlement, known as immediate or elastic settlement, occurs almost instantly upon application of structural loads. It is the reversible deformation caused by elastic strain in soil particles under stress redistribution *(Das, 2016).* It more significant in cohesionless soils (sands and gravels) and occurs within a few seconds to hours. It is independent of time and drainage.

The settlement generally occurs due to elastic compression of dry or partially saturated soils, rearrangement of particles or immediate stress transmission.

The settlement is expressed by the *Steinbrenner's (1934) and Fox's (1948)* equation relationship:

$$S_i = q_0 * \alpha * B' * \left(\frac{1-\mu_s}{E_s}\right) * I_f * I_s \qquad \text{Eq. 2.4}$$

Where:

S_i = immediate (elastic) settlement.

q_0 = net applied pressure on the foundation.

α = a factor that depends on the location (e.g., 4 for center, 1 for corner).

B' = minimum effective width of the loaded area.

E_s = average modulus of elasticity of the soil under the foundation.

μ_s = Poisson's ratio of the soil.

I_s = Steinbrenner's shape/influence factor (derived from Steinbrenner's 1934 work), which accounts for the shape of the foundation and the thickness of the compressible soil layer.

I_f = Fox's depth factor (from Fox's 1948 paper), which accounts for the foundation's embedment depth (D_f)

Settlement at the center of the foundation can be calculated using following values.

α = 4, m' = L/B, and n' = H / (B/2)

Settlement at the corner of the foundation can be calculated using following values.

α = 1, m = L/B, and n = H / B

2.3.2 Primary Consolidation

The primary consolidation stage represents the major phase of settlement in cohesive soils. It results from gradual expulsion of pore water under a constant applied load, which leads to an increase in effective stress and subsequent compression of the soil structure.

This process is time-dependent and governed by the Terzaghi one-dimensional consolidation theory (1943):

$$S_c = \frac{C_c}{1+ e_0} * H_0 * \log_{10}\left(\frac{\sigma_0' + \Delta\sigma}{\sigma_0'}\right) \quad \text{Eq. 2.5}$$

Where:

Cc = compression index,

e_0 = initial void ratio,

H0 = thickness of compressible layer,

σ0 = initial effective stress,

Δσ = increase in stress due to foundation load.

Mesri et al. identified permeability as a key soil property affecting the rate of volume change during consolidation, while compressibility influenced the magnitude of settlement and soil structure also played a role. Loading conditions, particularly the magnitude of applied pressure, directly influenced total vertical deformation and consolidation settlement. Drainage conditions and specimen

thickness effects were significant, with drainage paths and specimen thickness affecting the degree of consolidation achieved over time. Notably, *Al-Zoubi et al.* did not address specific influencing factors, focusing instead on methodological comparisons. Temperature and other environmental factors were not influencing factors in both cases.

Table 2.1 :- Factor affecting Primary Consolidation

Factor Category	**Specific Factors Identified**	**Relationships to Settlement Behavior**
Soil properties	Permeability, compressibility, structure	Permeability affects rate of volume change during consolidation; compressibility affects settlement magnitude
Loading conditions	Magnitude of applied pressure	Influences total vertical deformation and consolidation settlement
Drainage and specimen geometry	Drainage paths, specimen thickness	Affect degree of consolidation over time

2.3.3 Secondary Consolidation

The secondary consolidation stage, also called as creep settlement, occurs after the primary consolidation phase when excess pore pressures have dissipated and effective stress remains constant. Then the soil continues to compress slowly due to viscous rearrangement and slippage between soil particles.

The rate of secondary consolidation follows a logarithmic time relationship *(Mesri and Godlewski, 1977)*:

$$S_s = \frac{C_a}{1+e_0} * H_0 * \log_{10}\left(\frac{t_2}{t_1}\right) \quad \text{Eq. 2.6}$$

Where

C_a = secondary compression index, typically 2–10% of C_c for inorganic clays and 15–25% for organic clays.

$$C_a = \frac{\Delta e}{\log_{10}(t_2 / t_1)} \quad \text{Eq. 2.7}$$

Where

Δe = change in void ratio

t_1, t_2 = time

Tan et al.'s theoretical analysis revealed that water pressure and settlement during secondary consolidation are larger than predicted by Terzaghi's classical theory. Specifically, the ultimate settlement may be 1 to 3 times the maximal settlement predicted after Terzaghi's primary consolidation phase. This finding has significant implications for predicting long-term settlements in clay deposits.

Tan et al. described a gradual transition to ultimate settlement following the hydrodynamic period, while *Barber et al.* explicitly postulated this interrelation in their experimental work. However, *Barber et al.* noted that extrapolation of short-time tests to predict long-term secondary consolidation is uncertain, highlighting a practical limitation in predicting secondary consolidation behavior.

Tan et al. developed mathematical solutions for pore-water pressure and settlement using three-dimensional consolidation theory applied to laterally confined samples. The theoretical framework included rheological models to represent the physical behavior of clay layers. These mathematical expressions enabled prediction of cases ranging from low to high secondary compression, assuming negligible hardening effects.

The theoretical approach demonstrated that secondary consolidation calculations show water pressure and settlement consistently exceeding Terzaghi's predictions. The study emphasized that physical aspects and rheological models are essential for understanding the mathematical treatment of consolidation and secondary time effects.

Barber et al. focused on empirical observations and physical mechanisms rather than developing specific mathematical theories. Their work emphasized the role of hygroscopic moisture and material properties in secondary consolidation processes, providing experimental validation of the complex behaviors that theoretical models must account for.

Influencing Factors for Secondary Consolidation

1. Load Effects

Higher load magnitudes were found to accelerate the secondary consolidation process. *Barber et al.* measured the effects of various loads and precompression on secondary consolidation patterns, demonstrating that load magnitude is a critical factor in the rate of secondary compression.

2. Moisture and Hygroscopic Effects

Barber et al. identified hygroscopic moisture as the seat of secondary consolidation, based on tests conducted on desiccated, air-dry, and wet materials. The sorption of hygroscopic moisture was found to cause considerable swelling, representing a unique mechanism in secondary consolidation behavior. This finding suggests that moisture interactions at the particle scale play a fundamental role in time-dependent deformation.

3. Material Properties and Bonding

Tests on various materials including wood, rosin, and cotton revealed that bonding and creep of particles reduce secondary effects. Conversely, softening due to wetting causes large consolidations. These findings indicate that particle-level interactions and material structure significantly influence secondary consolidation magnitude and rate.

2.4 Time Rate Consolidation

Terzaghi's time-rate consolidation theory can be mathematically formulated through non-linear differential equations that linearize to include secondary consolidation effects, with the time factor-consolidation relationship represented as a rectangular hyperbola over the 60-90% consolidation range for practical engineering applications.

The time factor (T_v) defines the rate of settlement:

$$T_v = \frac{c_v * t}{d^2} \qquad \text{Eq. 2.8}$$

Where

C_v = coefficient of consolidation,

t = time elapsed.

d = drainage path length

The degree of consolidation (U) can then be approximated by:

$$U = 1 - \sum_{n=0}^{\infty} \frac{2}{\pi} \sin n\pi * e^{-n^2 \pi^2 T_v} \qquad \text{Eq. 2.9}$$

Relation between Tv and U is

$$Tv = (\Pi/4)\, U^2 \quad (\text{for } U \leq 0.60) \qquad \text{Eq. 2.10}$$

$$Tv = -0.933 \log_{10}(1-U) - 0.085 \quad (\text{for } U > 0.60) \qquad \text{Eq. 2.11}$$

The settlement at any time t can be calculated by,

$S_t = U * S_c$ Eq. 2.12

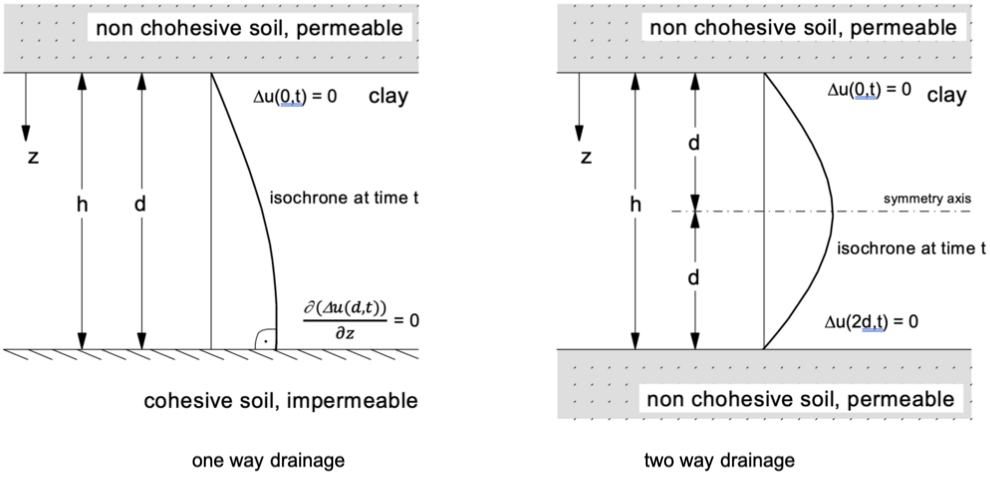

(Source: *www.ggu-software.com)*

Figure 2.2 :- Drainage Path in Consolidating Soil

Terzaghi's 1-D consolidation theory has fundamental limitations in its assumptions of linear stress-strain behavior and Darcy flow, resulting in significant prediction errors for fine-grained soils that necessitate modifications incorporating non-linear consolidation models and non-Darcy flow effects for accurate engineering applications.

2.5 Method of Settlement Analysis

Various approaches have been developed to estimate settlement, ranging from classical analytical solutions, empirical correlations, and laboratory-based tests to advanced numerical and finite element modeling. Each method offers specific advantages depending on soil characteristics, project scale, and data availability.

2.5.1 Analytical Method

The analytical method of settlement analysis is one of the oldest and most widely applied approaches in geotechnical engineering for estimating the vertical deformation of soil beneath foundations. It is based on theory-driven mathematical relationships that simplify complex soil behavior into manageable expressions using elasticity theory and one-dimensional consolidation theory. Analytical methods provide a first-level estimation of immediate, primary consolidation, and secondary settlements and are fundamental for the preliminary design of foundations *(Terzaghi, 1943; Bowles, 1996; Das, 2016)*.

2.5.2 Empirical Method

The empirical method of settlement analysis is based on observed field data, experimental correlations, and regression models that relate measurable soil properties to foundation performance. Unlike purely theoretical analytical methods, empirical approaches rely on statistical relationships developed from in-situ tests, laboratory experiments, and field measurements over decades of engineering practice.

Empirical methods are particularly valuable where detailed soil models are unavailable or where the soil profile exhibits variability and complexity, as in the Kathmandu Valley, characterized by heterogeneous silty clay and sandy silt layers. These methods provide quick, reliable settlement estimates during preliminary design and serve as a practical complement to analytical and numerical approaches *(Bowles, 1996; Peck et al., 1974; Das, 2016)*.

2.5.3 Janbu method of Settlement Calculation

Janbu, Bjerrum, and Kjaernsli (1956) made a significant contribution to the prediction of immediate settlement of shallow foundations, particularly for flexible foundations resting on saturated clay soils. Their work is widely regarded as a foundational development in geotechnical engineering, as it combines theoretical elasticity solutions with empirical modifications to better represent field conditions.

The authors proposed a simplified method to estimate the average settlement of flexible foundations by introducing dimensionless correction factors into the classical elastic settlement equation. The general expression is given as:

$$S_e = A_1 A_2 \frac{q_0 B}{E_s} \qquad \text{Eq. 2.13}$$

Where

S_e is the elastic settlement,

q_0 is the applied net pressure,

B is the foundation width,

Es is the soil modulus and

A_1 and A_2 are correction coefficients that account for foundation geometry and embedment conditions.

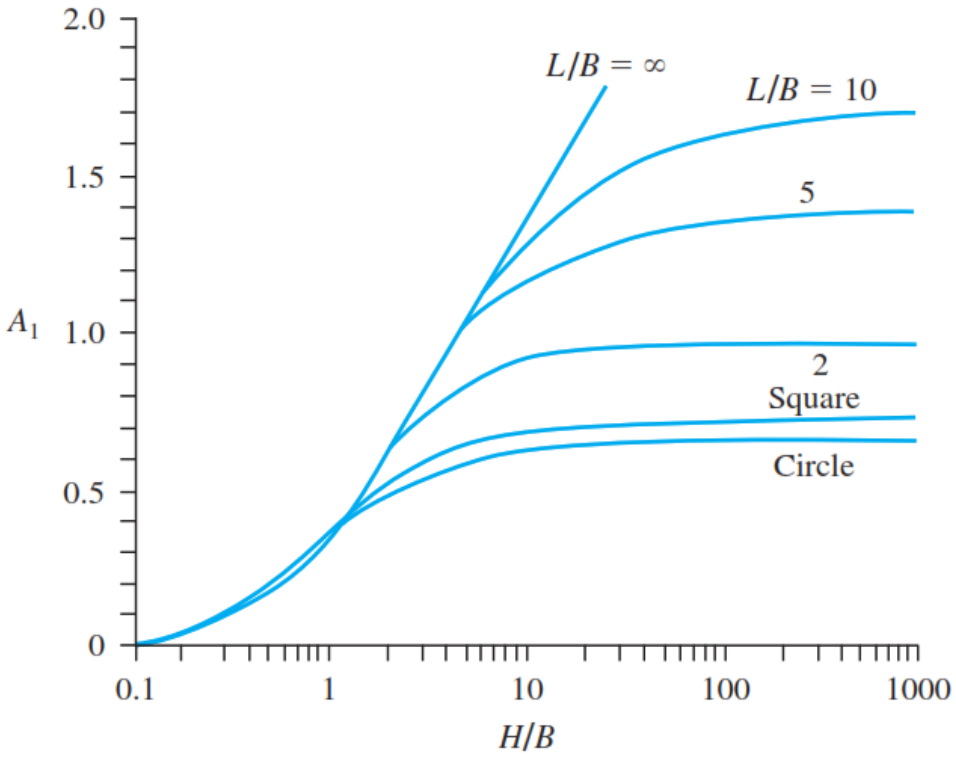

(Source: - *Christian, J. T., & Carrier III, W. D. (1978). Janbu, Bjerrum and Kjaernsli's chart reinterpreted)*

Figure 2.3 :- Values of A_1 for elastic settlement calculation

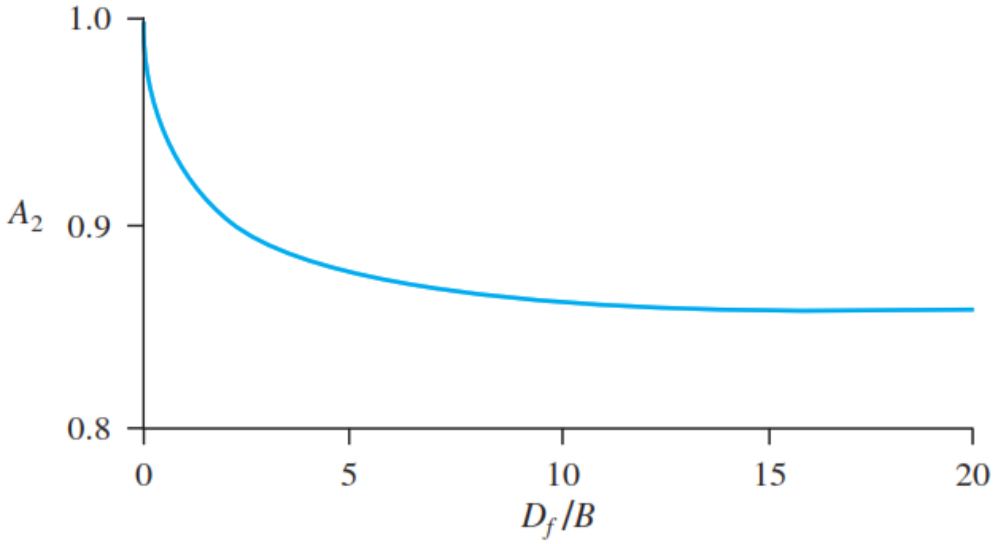

(Source: - *Christian, J. T., & Carrier III, W. D. (1978). Janbu, Bjerrum and Kjaernsli's chart reinterpreted)*

Figure 2.4 :- Values of A_2 for elastic settlement calculation

A key feature of the *Janbu et al. (1956)* method is the introduction of chart-based correction factors. The factor A_1 incorporates the effects of foundation shape and the thickness of the compressible soil layer, expressed through ratios such as L/B (length-to-width) and H/B (depth to rigid layer). The factor A_2 accounts for the

depth of embedment (D_f/B), reflecting the reduction in settlement with increasing foundation depth. These charts were developed based on elastic theory and calibrated using practical observations, making the method suitable for engineering applications.

This method assumes that the soil acts as a linear elastic, homogeneous, and isotropic material with a Poisson's ratio close to 0.5, which corresponds to undrained conditions in saturated clays. Furthermore, the foundation is believed to be completely flexible, which results in homogeneous contact pressure distribution. These assumptions simplify the study, but they may limit the method's usefulness in highly nonlinear or layered soil conditions.

2.5.4 Numerical Modelling

Numerical modeling has become an essential tool in modern geotechnical engineering for analyzing the settlement behavior of soil–foundation systems. Traditional analytical and empirical methods, though widely used, often rely on simplifying assumptions that neglect the nonlinear, heterogeneous, and anisotropic behavior of soils. In contrast, numerical methods particularly the Finite Element Method (FEM) and Finite Difference Method (FDM) allow for a more accurate simulation of soil response under various loading conditions.

Among the software tools available, PLAXIS 3D has gained prominence for its ability to model three-dimensional stress–strain behavior, staged construction, and soil–structure interaction (SSI). Numerical modeling enables engineers to visualize stress distribution, pore pressure variation, and settlement evolution over time, offering a detailed understanding of foundation performance.

The governing equilibrium equation in FEM for soil deformation is:

$$[K]\{u\} = \{F\} \qquad \text{Eq. 2.14}$$

Where,

[K] = global stiffness matrix,

{u}= nodal displacement vector,

{F}= external load vector.

This equation is solved iteratively to obtain displacement and stress fields across the soil continuum. Settlement at any node can then be extracted from the computed vertical displacements.

2.6 PLAXIS 3D

PLAXIS 3D is a finite element–based numerical software developed for analyzing the deformation and stability of soil and rock structures under various loading and boundary conditions. It provides a robust three-dimensional (3D) framework for settlement analysis, enabling engineers to capture the realistic stress–strain response of complex soil–structure systems that cannot be adequately modeled using traditional analytical or empirical methods.

The settlement of a foundation is influenced by factors such as soil stiffness, compressibility, load intensity, groundwater conditions, and construction sequence. In complex urban settings like Kathmandu Valley, where heterogeneous silty clays and sandy layers are prevalent, 3D modeling is essential for accurately representing soil behavior beneath large-scale commercial structures such as Labim Mall.

PLAXIS 3D simulates the interaction between foundation elements (e.g., raft, piles) and surrounding soils by incorporating advanced constitutive soil models, staged loading, and drainage/consolidation effects, allowing a more realistic assessment of total and differential settlement.

In PLAXIS 3D, the process of settlement analysis involves three main stages input, calculation, and output, each of which plays a crucial role in achieving accurate and realistic simulation results.

2.6.1 Input

The input stage begins with defining the overall geometry of the soil domain and foundation system. The model is created to represent the actual field conditions, ensuring that the soil domain extends sufficiently in all directions to avoid boundary effects. Site-specific geotechnical data, such as borehole logs, are used to define the soil stratigraphy, and each layer is assigned a suitable constitutive model such as Mohr–Coulomb or Hardening Soil (HS) depending on soil behavior and the required accuracy. The material properties include stiffness modulus (E_{50}), cohesion (c), internal friction angle (ϕ), Poisson's ratio (ν), unit weight (γ), and permeability (k), which are obtained from laboratory and field tests. Proper boundary conditions are then set fixing the bottom in all directions and restraining lateral boundaries horizontally while loads are applied as uniform surface pressures or as structural elements to simulate real building loads. The model is discretized into a finite element mesh, with finer elements under the foundation to capture stress concentration and deformation more precisely.

2.6.2 Calculation

Once all inputs are defined, the calculation stage is initiated. PLAXIS 3D employs the finite element method (FEM) to solve the soil–structure interaction problem numerically. Depending on the objective, different analysis types such as plastic analysis, consolidation analysis is chosen. The program calculates displacements, stresses, and pore pressures in each element using incremental-iterative procedures like the Newton–Raphson method until equilibrium is achieved. For consolidation problems, time-dependent behavior is simulated to capture the gradual dissipation of pore water pressure and the corresponding primary settlement. The staged construction option allows simulation of progressive loading, excavation, or construction sequences to replicate actual field conditions.

2.6.3 Output

The output stage provides a range of numerical and graphical results that describe the deformation and stress response of the soil and foundation system. The primary outputs include total settlement, differential settlement, and vertical and horizontal displacements. PLAXIS also generates contour plots showing the distribution of stresses, strains, and pore pressures within the soil mass, allowing visualization of critical zones beneath the foundation. Time–settlement curves and pore pressure dissipation graphs illustrate the rate and magnitude of consolidation settlement. These outputs can be validated by comparing them with analytical results or field measurements from plate load tests and settlement monitoring. In summary, the input phase establishes the physical and mechanical model, the calculation phase performs numerical simulation based on finite element theory, and the output phase interprets the resulting deformations, stresses, and settlements—together providing a complete and reliable understanding of foundation performance under load.

2.7 Case Study of ICT Building, Pulchowk

The practice continuous regarding of settlement of structure have been carried out since hundreds of years in outside of Nepal. In context of Nepal, Settlement observations and analysis of ICT center building, Pulchowk was carried out by *Devkota, P. (2018)* and the total settlement was found out to be 258 mm and in upto sixth year of its construction settlement was upto 236 mm.

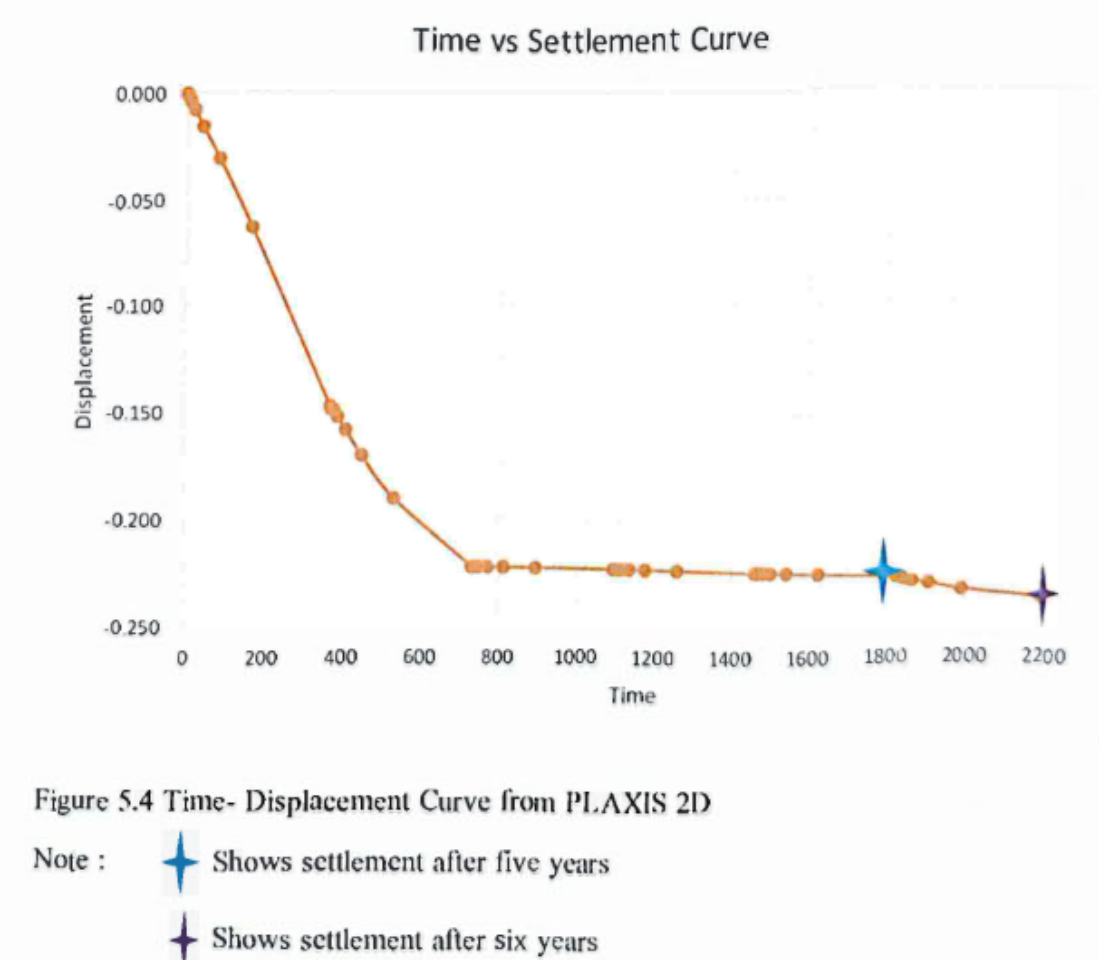

(Source: - *Devkota, P. (2018) Settlement observation and analysis of ICT Pulchowk)*

Figure 2.5 :- Settlement Curve of ICT Building

3 SOIL AND BUILDING PROPERTIES

3.1 Introduction

The mall is constructed is located on grey silt of medium stiff of low plasticity at Pulchowk, Lalitpur. The SPT test were executed at five places over there. The properties of the soil have been obtained from the borehole profile along with SPT values are shown in **Appendix - A** . Soil investigation work was performed by Central Material Testing Laboratory (CMTL), Pulchowk, Lalitpur in 2002 for the purpose of design of foundation of the building. Five boreholes have been drilled at the location designated as BH1, BH2, BH3, BH4 and BH5 upto depth of 30m. The results of the soil investigation have been compiles in soil investigation report prepared by *CMTL (2002)*, of which data has been used for this study. All the boreholes were considered for settlement analysis of Labim Mall as all borehole have similar data regarding SPT values, specific weight and moisture content.

Table 3.1 :- Summary of Field Works from CMTL (2002)

S. N.	Boring Type	Borehole No.	Date	Depth (m)
1	Percussion Boring	1	Aug 17, 2002	30
2	Percussion Boring	2	Aug 30, 2002	30
3	Percussion Boring	3	Sept 3, 2002	30
4	Percussion Boring	4	Aug 26, 2002	30
5	Percussion Boring	5	Aug 22, 2002	30

(Source: - *CMTL (2002))*

During SPT test, several factors contribute to the variation of the standard penetration number N at a given depth for similar soil profiles. Among these factors to be considered are SPT hammer efficiency, borehole diameter, sampling method and rod length *(Skempton, 1986).*

3.2 Properties of Soil

The properties of soil of all borehole are shown in **Appendix - A** . The borehole logs show that the ground water table lies within 1m from ground surface. The soil consists of dark grey to grey silt of medium stiff to stiff of low plasticity upto 16m depth then dark grey stiff organic clay of high plasticity upto 30m.

3.3 Nature of Building

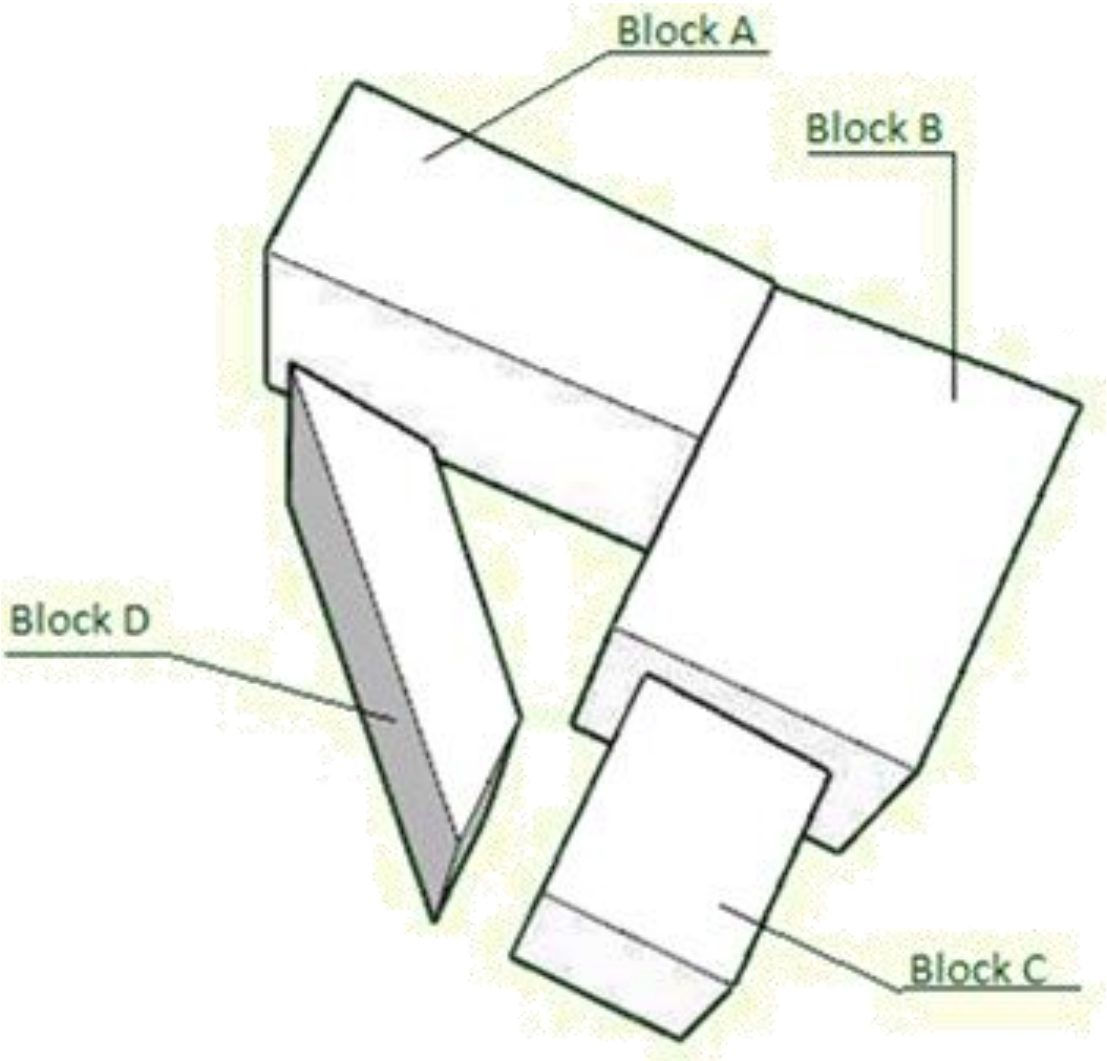

Figure 3.1 :- Layout of Labim Mall

3.3.1 Superstructure

The building whose settlement is being analyzed is situated in Pulchowk, Lalitpur. It is a five storied building with double basement. The total area of floor area of building is 210142.15 ft^2 and total height of building is 106 ft 10 in. the building comprises of our blocks labelled as Block A, Block B, Block C and Block D as per the Figure 3.1. each block are separated by a seismic gap joint of 6 in. The floor plan is shown in Figure 3.2. And the size of raft footing of each block is different.

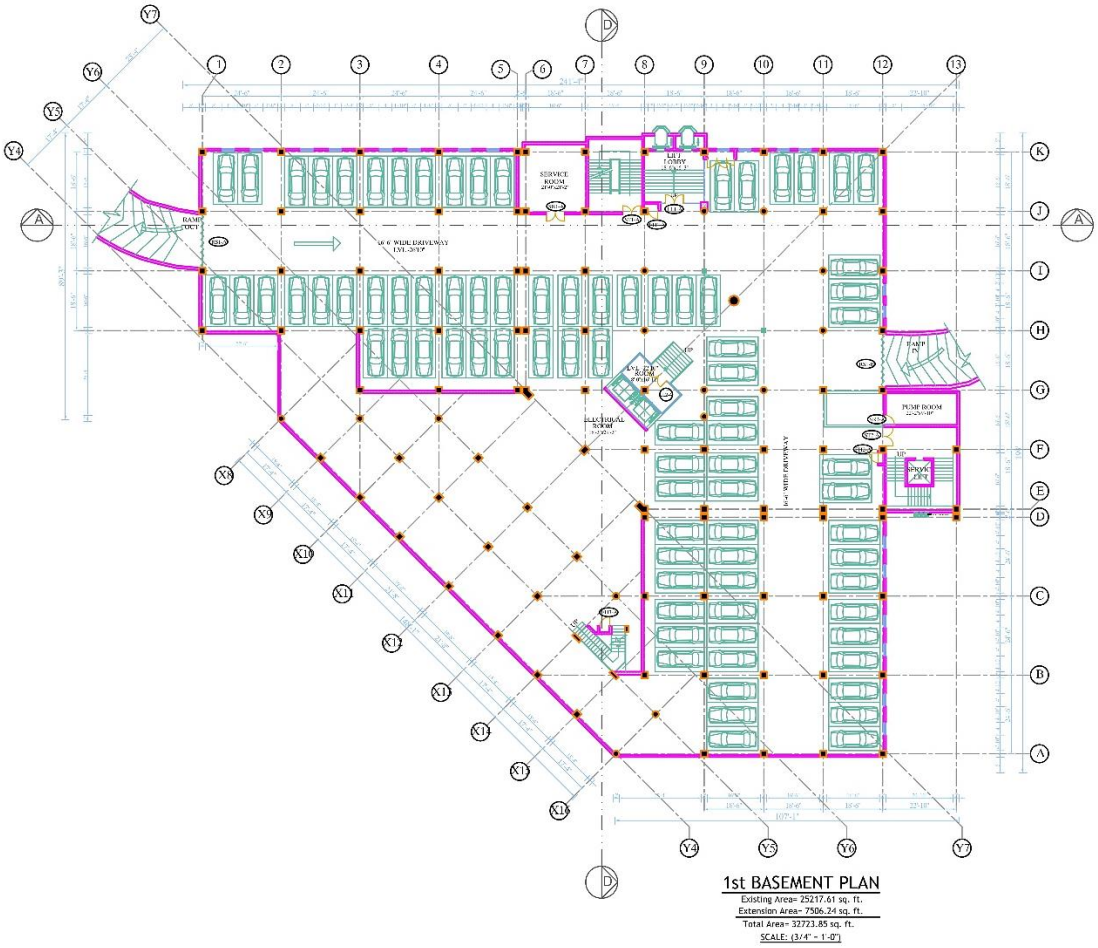

Figure 3.2 :- Plan of Labim Mall

3.3.2 Foundation

The four blocks are standing on a raft foundation laid at a depth of 4m below the existing ground surface. The raft covers the entire floor plan of the building. It is assumed that uniform stress passes through the raft foundation to the soil all over the area. The foundation detail of all blocks are as follows:

Table 3.2 :- Building Foundation Details

Block	Foundation Type	Thickness (ft)	Effective Area (ft^2)	Effective Length	Effective Breadth
Block A	Raft	3'3''	8925	100''	89'3''
Block B	Raft	3'3''	13032.67	115'4''	113''
Block C	Raft	3'3''	5586	76'	73'6''
Block D	Raft	3'	5869.72	160'1	36'8''

3.3.3 Construction

The soil test on Labim mall site was done in 2002 September. However, the construction of Labim mall occurred in two phases where in first phase Block A, B and C were constructed and in second phase Block D was constructed. Construction of first phase building Block A, B and C started in 2007 March and of second phase building Block D started in 2015 April.

The difference in construction period of different block has been taken into consideration during the settlement analysis by PLAXIS-3D. So, the time period for Phase 1 is taken as 2,953 days and Phase 2 is taken as 3,787 days totaling 6,740 days.

4 METHOD OF ANALYSIS

4.1 Introduction

This chapter contains the description of method of analysis to predict the settlement of the building. Common practice in foundation design is to limit the amount of settlement, i.e. the maximum settlement experienced by the building. In the saturated cohesive soil, the prediction of settlement must at least include that of consolidation settlement since it is generally the dominating component in this type of soil. hen an external pressure is applied to a saturated clay-water system, the water in the pores initially absorbs the pressure, leading to an excess pore water pressure drainage that exceeds the surrounding hydrostatic water pressure of the clay mass. With the passage of time, the excess pore pressure dissipates to the drainage surface and the soil begins to compress. Consolidation is the process of gradually compressing soil while also allowing pore water to flow out of the soil mass and gradually transferring applied load from the pore water to the mineral skeleton. Consolidation continues until the excess pore water pressure has completely dissipated and the pore pressure returns to hydrostatic, a process that in cohesive soils takes a large amount of time, and hence the potential of creating post- construction problems.

Two major concerns in the consolidation of cohesive soils are therefore the amount of settlement at the end of consolidation, or the primary consolidation settlement, and the rate of consolidation with respect to time. This chapter will discuss how these two main aspects of consolidation are treated for the case of the building in study.

4.2 Consolidation

The term primary consolidation settlement refers to the final settlement at the end of the primary consolidation when the soil is subjected to a load. The primary consolidation is function of the compression properties of the soil and does not depend on whether the load is applied instantaneously or gradually. As mentioned earlier in Section 2.3.2 the Primary Consolidation settlement of a thick deposit or of multi layered soil.

The change in void ratio (Δe) can be expressed in terms of the compression index (C_c) for normally consolidated soils. However, the initial effective stress is a variable which changes as per the depth of clay layers, and is necessary to define

the value representing the relevant layer of that depth. The resulting settlement is altered greatly depending on the defined value.

$$S_c = \frac{C_c}{1+e_0} * H_0 * \log_{10}\left(\frac{\sigma_0' + \Delta\sigma}{\sigma_0'}\right) \quad \text{Eq. 4.1}$$

Where:

C_c = compression index,

e_o = initial void ratio,

H_0 = thickness of compressible layer,

σ_0 = initial effective stress,

$\Delta\sigma$ = increase in stress due to foundation load.

4.3 Thickness of Consolidating Layer

One of the first steps of settlement is to determine the thickness of the consolidating layer. For a thick deposit, this is normally decided by analyzing the extent of the pressure imposed by the load on the sub-soil. A value of 10% of imposed pressure on the ground is generally considered small enough for consideration to be ignored. Hence the distribution of the vertical stress imposed by the building through the depth of the subsoil should first be determined to find the extent of the pressure bulbs to a stress level equal to 10 % of the applied pressure on the surface.

Various stress distribution charts based on theory of elasticity are available in the literature. These standard charts are available only for the regular shapes of uniformly distributed load such as rectangular, circular and strip loading. Since none of these standard charts is applicable for the building in this study, the distribution of vertical stress is calculated with the help of Newmark's Chart.

For this study, since the building covers large area and due to its excessive load vertical stress would be developed to a greater depth. But the death of bore hole is only 30m so the data is not available below this depth. This 30m depth in this analysis is assumed as the thickness of the compressible layer under the foundation of the building.

4.4 Soil Layer Division

Consolidation analysis of a thick layer extending from the ground surface to a deep depth requires that the soil be divided into thinner sub layers to accommodate the

varying parameters across the depth as well as the fact that the variation of the vertical stresses with depth is not linear.

From the laboratory test data, the soils at all depth of bore hole are almost homogeneous i.e of dark grey to grey silt of medium stiff to stiff of low plasticity upto 16m depth then dark grey stiff organic clay of high plasticity upto 30m, but other properties are different throughout the depth. So, the layer of soil can be divided into thinner sub-layer of 2 m thick. If the consolidating layer is divided into smaller sub layer, the total consolidation settlement of the consolidation layer is the summation of the settlement of sub-layers. For the soil having multiple layers for the calculation of the initial effective stress of each layer, and to calculate the consolidation settlement based on such results, as given in Eq.

$$S_c = \sum_{i=1}^{n} \left(\frac{C_c}{1+e_0} * H_0 * \log_{10} \left(\frac{\sigma_0' + \Delta\sigma}{\sigma_0'} \right) \right) \qquad \text{Eq. 4.2}$$

Where, n is the number of layers

In Equation 4.2 e_0 should be determined from the relevant (e, log σ_v) graph of the soil layer and the change of stresses can be determined from 2:1 vertical distribution method for the depth.

The consolidation test and graph of (e, log σ_v) of BH 1 and sample UD1 and UD4 are tabulated below:

Table 4.1 :- Consolidation Test of UD-1 of BH1

CONSOLIDATION TEST

Location: Pulchowk, Laitpur
Sample:- UD-1 **Depth:-** 7 m

Wt. of Ring + Wet soil, gm	:	283.08	Initial moisture content (w) , %	:	33.20
Wt. of Ring + Dry soil, gm	:	241.81	Initial void ratio, eo = w.G	:	0.867
Wt. of Ring, gm	:	117.50	Specific Gravity of solids (G)	:	2.610
Ht. of solids, Ho = [ho/(1+eo)], mm	:	10.72	Initial height of sample (ho), mm	:	20.00

Pressure Intensity (kN/sq.m)	**3.00**	**6.00**	**12.00**	**24.00**	**48.00**	**96.00**	**192.00**	**384.00**	**192.00**	**3.00**
Elapsed Time (minutes)	Dial Gauge Reading									
0	2500.0	2482.0	2472.0	2456.0	2428.5	2408.0	2367.0	2322.5	2271.0	2278.0
0.5	2492.0	2480.0	2468.0	2445.0	2420.0	2390.0	2339.0	2291.0		
1	2489.5	2479.0	2465.0	2442.0	2418.5	2385.0	2335.0	2286.0		
2	2489.0	2477.0	2463.0	2439.0	2417.5	2380.0	2334.0	2284.0		
3	2488.5	2476.5	2462.0	2437.0	2416.5	2378.0	2334.0	2283.5		
4	2488.0	2476.0	2461.5	2436.0	2416.0	2376.5	2333.5	2282.0		
8	2487.5	2475.5	2461.0	2435.5	2415.0	2375.5	2332.5	2281.5		
16	2486.5	2475.0	2460.5	2434.0	2414.5	2374.5	2331.5	2280.5		
30	2485.5	2475.0	2460.0	2433.5	2414.0	2373.0	2329.5	2279.0	2278.0	2348.0
60	2485.0	2474.5	2459.0	2432.5	2412.0	2372.0	2327.5	2277.5		
120	2484.5	2474.0	2459.0	2432.0	2411.0	2370.5	2326.5	2276.0		
240	2483.5	2473.0	2458.0	2430.5	2410.0	2369.0	2324.0	2273.5		
1440	2482.0	2472.0	2456.0	2428.5	2408.0	2367.0	2322.5	2271.0		

Pressure Intensity kN/sq.m.	**Dial Reading**	**Change in height mm.**	**Ht. of sample mm.[2H]**	**Equiv. ht. of voids [2H-Ho]**	**Void ratio e=(2H-2Ho)/2Ho**	**m_v m²/kN**
0	2500	-	20.00	9.28	0.87	
3	2482	0.18	19.82	9.10	0.85	3.00E-03
6	2472	0.28	19.72	9.00	0.84	1.67E-03
12	2456	0.44	19.56	8.84	0.83	1.33E-03
24	2429	0.72	19.29	8.57	0.80	1.15E-03
48	2408	0.92	19.08	8.36	0.78	4.27E-04
96	2367	1.33	18.67	7.95	0.74	4.27E-04
192	2323	1.78	18.23	7.51	0.70	2.32E-04
384	2271	2.29	17.71	6.99	0.65	1.34E-04
192	2278	2.22	17.78	7.06	0.66	1.82E-05
3	2348	1.52	18.48	7.76	0.72	1.85E-04

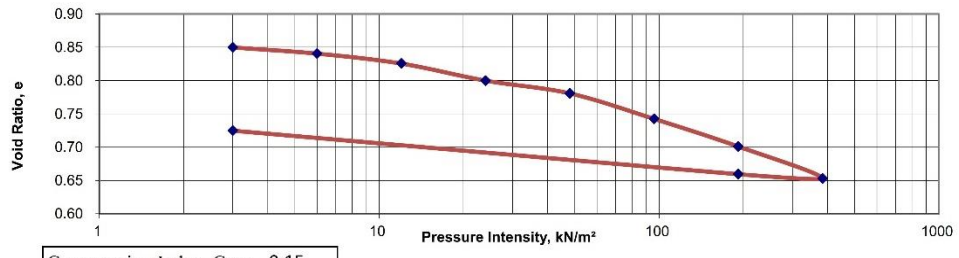

Compression Index, Cc = 0.15

(Source: - *CMTL (2002)*)

Table 4.2 :- Consolidation Test of UD-4 of BH1

CONSOLIDATION TEST

Location: Pulchowk, Laitpur
Sample:- UD-4 **Depth:-** 24 m

Wt. of Ring + Wet soil, gm	:	241.73	Initial moisture content (w) , %	:	89.06
Wt. of Ring + Dry soil, gm	:	183.21	Initial void ratio, eo = w.G	:	2.200
Wt. of Ring, gm	:	117.50	Specific Gravity of solids (G)	:	2.470
Ht. of solids, Ho = [ho/(1+eo)], mm	:	6.25	Initial height of sample (ho), mm	:	20.00

Pressure Intensity (kN/sq.m)	**3.00**	**6.00**	**12.00**	**24.00**	**48.00**	**96.00**	**192.00**	**384.00**	**192.00**	**3.00**
Elapsed Time (minutes)	Dial Gauge Reading									
0	2450.0	2433.0	2402.0	2332.0	2234.0	2065.0	1859.0	1406.0	830.0	898.0
0.5	2440.0	2420.0	2375.0	2295.0	2148.0	1955.0		1260.0		
1	2438.0	2418.0	2358.0	2289.0	2142.0	1945.0	1740.0	1230.0		
2	2435.5	2417.0	2356.0	2284.0	2136.0	1935.0	1692.0	1202.0		
3	2435.0	2416.0	2354.0	2280.0	3132.0	1931.0	1670.0	1170.0		
4	2434.0	2415.0	2353.0	2275.0	2127.0	1927.0	1660.0	1142.0		
8	2433.5	2413.5	2351.0	2271.0	2121.0	1923.0	1642.0	1127.0		
16	2433.0	2413.0	2349.0	2269.0	2110.0	1919.0	1590.0	1090.0		
30	2433.0	2412.0	2347.0	2260.0	2098.0	1907.0	1518.0	1068.0	898.0	1242.0
60	2433.0	2411.0	2345.0	2256.0	2091.5	1898.0	1490.0	1005.0		
120	2433.0	2409.5	2342.5	2250.0	2086.0	1887.0	1465.0	950.0		
240	2433.0	2407.5	2339.0	2245.0	2080.0	1879.0	1447.0	912.0		
1440	2433.0	2402.0	2332.0	2234.0	2065.0	1859.0	1406.0	830.0		

Pressure Intensity kN/sq.m.	**Dial Reading**	**Change in height mm.**	**Ht. of sample mm. [2H]**	**Equiv. ht. of voids [2H-Ho]**	**Void ratio e= (2H-2Ho)/2Ho**	**m_v m²/kN**
0	2450	-	20.00	13.75	2.20	
3	2433	0.03	19.97	13.72	2.19	5.67E-04
6	2402	0.10	19.90	13.65	2.18	1.03E-03
12	2332	0.24	19.76	13.51	2.16	1.17E-03
24	2234	0.43	19.57	13.32	2.13	8.17E-04
48	2065	0.77	19.23	12.98	2.08	7.04E-04
96	1859	1.18	18.82	12.57	2.01	4.29E-04
192	1406	2.09	17.91	11.66	1.87	4.72E-04
384	830	3.24	16.76	10.51	1.68	3.00E-04
192	898	3.10	16.90	10.65	1.70	3.54E-05
3	1242	2.42	17.58	11.33	1.81	1.82E-04

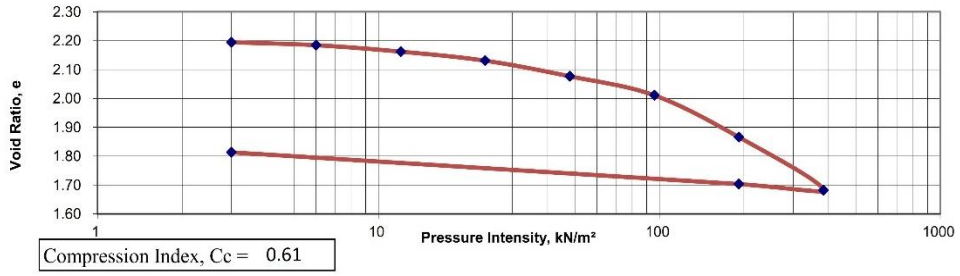

Compression Index, Cc = 0.61

(Source: - *CMTL (2002)*)

4.5 Time Rate Consolidation

The final settlement of a structure is not the only concern that an engineer faces in consolidation analysis. The progress of consolidation is another important aspect in consolidation that governs the rate of settlement with time, which gives an idea about how fast the structure is settling and how much time is required for the

structure to seize settling considerably, a process that may take many years depending on the nature of the soil. It emphasizes the stage of soil in consolidation or settlement stages either primary or secondary. The finite difference method is used in this study to estimate the time settlement -time characteristics of the building.

4.6 Selection of Consolidation Parameters

As already described in Section 4.2 the death of bore hole is only 30m and the data is not available below this depth. In this analysis 30m depth is assumed as the thickness of the compressible layer under the foundation of the building. Because of the excavation approximately 4m to place the raft foundation suggested by soil investigation report of ICT Center building, *CMTL (2002)*. So, the soil parameter needed for the analysis must be determine from depths 4m and 30m. During soil investigation work of the site prior to the construction of building, undisturbed samples have been collected at every 1.5 m. The samples have been subjected to different soil tests. The coefficient of consolidation C_v has been determined from the square root time method for on every incremental load and taking the average value only, since the same parameters could not be determined from log-time method due to the unconventional shape of the graph. Time factor (T_v) has been calculated using the relationship given below:

$$T_v = \frac{c_v * t}{d^2} \qquad \text{Eq. 4.3}$$

Where

C_v = coefficient of consolidation,

t = time elapsed.

d = drainage path length

The degree of consolidation (U) can be determined by using the following relationship,

$Tv = (\Pi/4)\, U^2$ (for $U \leq 0.60$) Eq. 4.4

$Tv = -0.933 \log_{10}(1-U) - 0.085$ (for $U > 0.60$) Eq. 4.5

4.7 Modelling in Plaxis-3D

The finite element method is the most used method for analysis in engineering works. PLAXIS 3D software is a finite element tool which is used for geotechnical works. Soil is a material that exhibits different behavior when it is loaded,

unloaded, and reloaded. PLAXIS 3D software used in this research to simulate the soil behavior under raft foundation for different nature and loads. It can simulate stress development, deformation, consolidation, or stability. And, results such as displacements, settlements, stresses, safety factors, and flow patterns are interpreted to support design decisions and verify geotechnical performance.

4.7.1 Project Properties

The finite element soil geometry model adopted for the analysis of raft foundation of dimension of different blocks, and the added stress of column loads. The soil models used in the software was linear elastic model for grey silt of medium stiff to stiff for the settlement analysis. After the creation of the geometry of the three-dimensional (3D) model of (115m * 100m * 30m) the mesh were generated automatically for every borehole log.

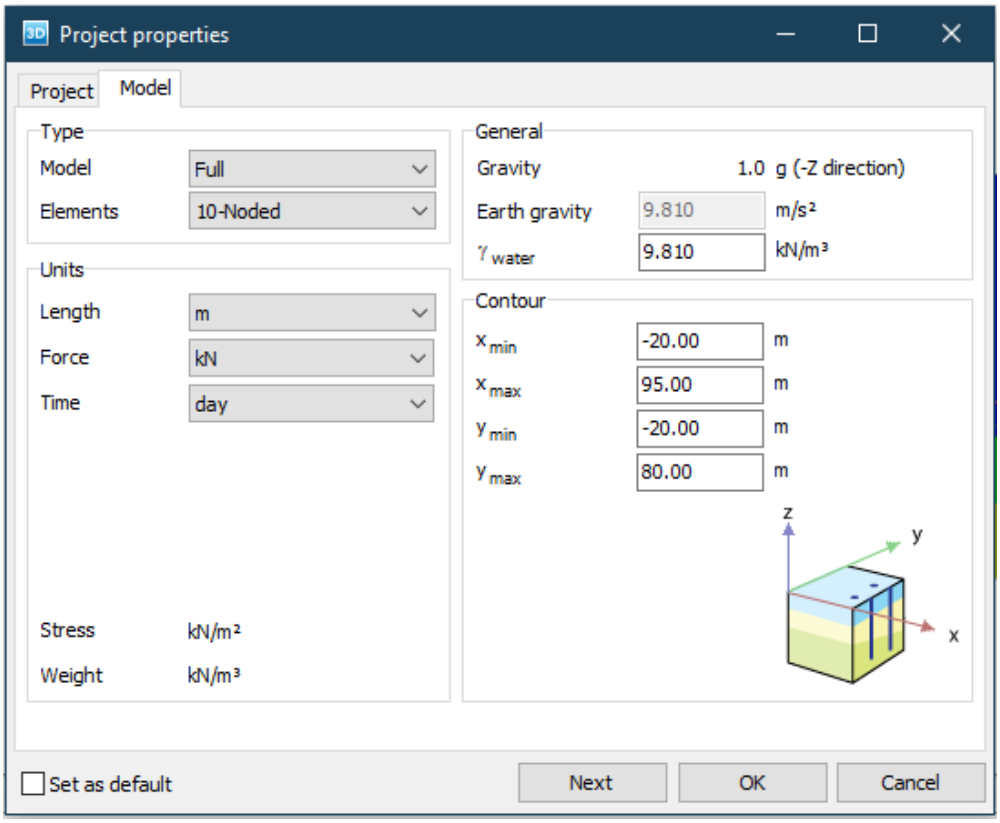

Figure 4.1 :- Project Properties

4.7.2 Soil Properties

The modelling process starts with defining the project properties that control numerical behavior and groundwater conditions relevant to settlement prediction i.e, soil present at below the building. The soil is of dark grey to grey silt of medium stiff to stiff of low plasticity upto 16m depth then dark grey stiff organic clay of

high plasticity upto 30m of BH1 and consecutively of other boreholes too. Initial water table are specified to ensure realistic stress and pore-pressure initialization. Soil materials are assigned using appropriate constitutive Mohr-Colomb model. The general properties of soil of all Boreholes are listed below:

Table 4.3 :- Soil Material Properties of Borehole 1

Parameter	**Symbol**	**Borehole 1**		**Unit**
		Upper Soil	**Lower Soil**	
Property	-	Mohr-Colomb	Mohr-Colomb	-
Unsaturated Weight	Υ_{unsat}	17.5	12	kN/m^3
Saturated Weight	Υ_{sat}	18.64	15.01	kN/m^3
Modulus of Elasticity	E’	31.88E3	44.15E3	kN/m^2
Poisson’s Ratio	ν'	0.3	0.25	-
Cohesion	c'	11	20	kN/m^2
Friction Angle	Φ’	21.8	24.25	Degree
Thickness	D	2-16	16-30	m

Table 4.4 :- Soil Material Properties of Borehole 2

Parameter	**Symbol**	**Borehole 2**		**Unit**
		Upper Soil	**Lower Soil**	
Property	-	Mohr-Colomb	Mohr-Colomb	-
Unsaturated Weight	Υ_{unsat}	17.5	12.5	kN/m^3
Saturated Weight	Υ_{sat}	17.99	14.27	kN/m^3
Modulus of Elasticity	E’	35E3	40.01E3	kN/m^2
Poisson’s Ratio	ν'	0.3	0.25	-
Cohesion	c'	13.5	20	kN/m^2
Friction Angle	Φ’	24.23	22.42	Degree
Thickness	D	2-16	16-30	m

Table 4.5 :- Soil Material Properties of Borehole 3

Parameter	Symbol	Borehole 3		Unit
		Upper Soil	Lower Soil	
Property	-	Mohr-Colomb	Mohr-Colomb	-
Unsaturated Weight	Υ_{unsat}	17.5	12.5	kN/m^3
Saturated Weight	Υ_{sat}	21.29	15.11	kN/m^3
Modulus of Elasticity	E’	31.87E3	40.61E3	kN/m^2
Poisson’s Ratio	ν'	0.3	0.25	-
Cohesion	c'	19	22.5	kN/m^2
Friction Angle	Φ’	19.93	31.09	Degree
Thickness	D	2-16	16-30	m

Table 4.6 :- Soil Material Properties of Borehole 4

Parameter	Symbol	Borehole 4		Unit
		Upper Soil	Lower Soil	
Property	-	Mohr-Colomb	Mohr-Colomb	-
Unsaturated Weight	Υ_{unsat}	17.5	12.5	kN/m^3
Saturated Weight	Υ_{sat}	19.32	14.81	kN/m^3
Modulus of Elasticity	E’	32.88E3	37.96E3	kN/m^2
Poisson’s Ratio	ν'	0.3	0.25	-
Cohesion	c'	10.96	20	kN/m^2
Friction Angle	Φ’	21.8	20.1	Degree
Thickness	D	2-17	17-30	m

Table 4.7 :- Soil Material Properties of Borehole 5

Parameter	Symbol	Borehole 5		Unit
		Upper Soil	Lower Soil	
Property	-	Mohr-Colomb	Mohr-Colomb	-
Unsaturated Weight	Υ_{unsat}	17.5	13.5	kN/m^3
Saturated Weight	Υ_{sat}	19.13	15.5	kN/m^3
Modulus of Elasticity	E'	24.53E3	36.79E3	kN/m^2
Poisson's Ratio	ν'	0.3	0.25	-
Cohesion	c'	16	15	kN/m^2
Friction Angle	Φ'	25.4	33.02	Degree
Thickness	D	2-15	15-30	m

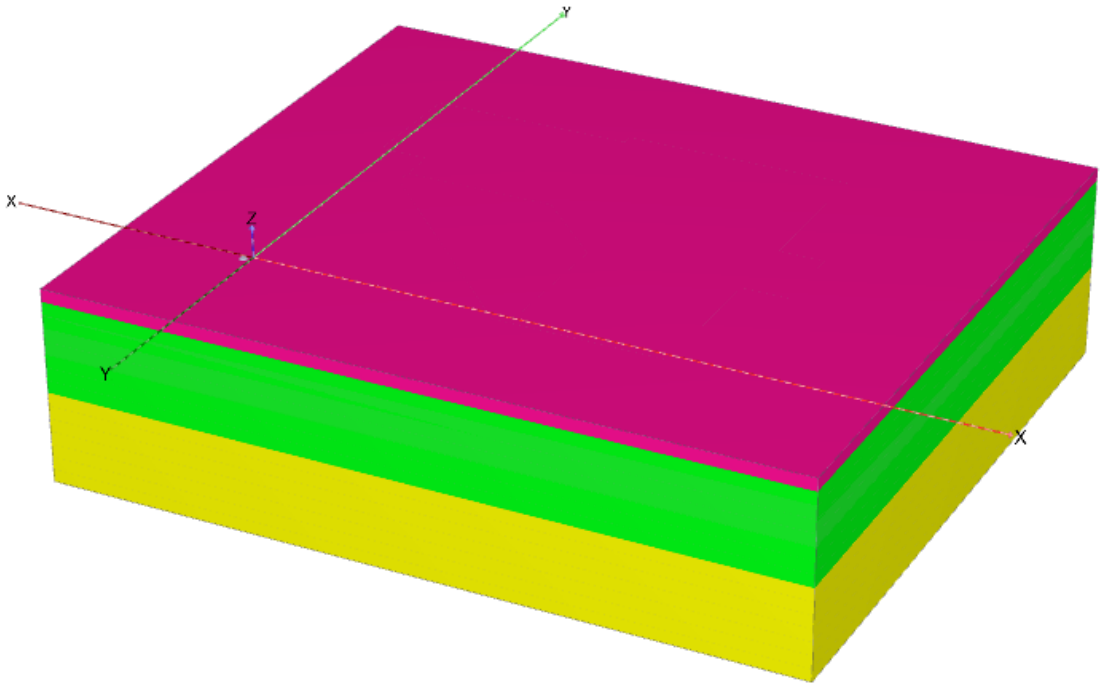

Figure 4.2 :- Different Soil Layers

4.7.3 Mesh Generation

For the calculation, the whole soil structure has been divided into elements. In order to analyze the influence of mesh medium coarseness has been applied. Finer the mesh more time consumption so the medium coarseness value of 0.5 is taken.

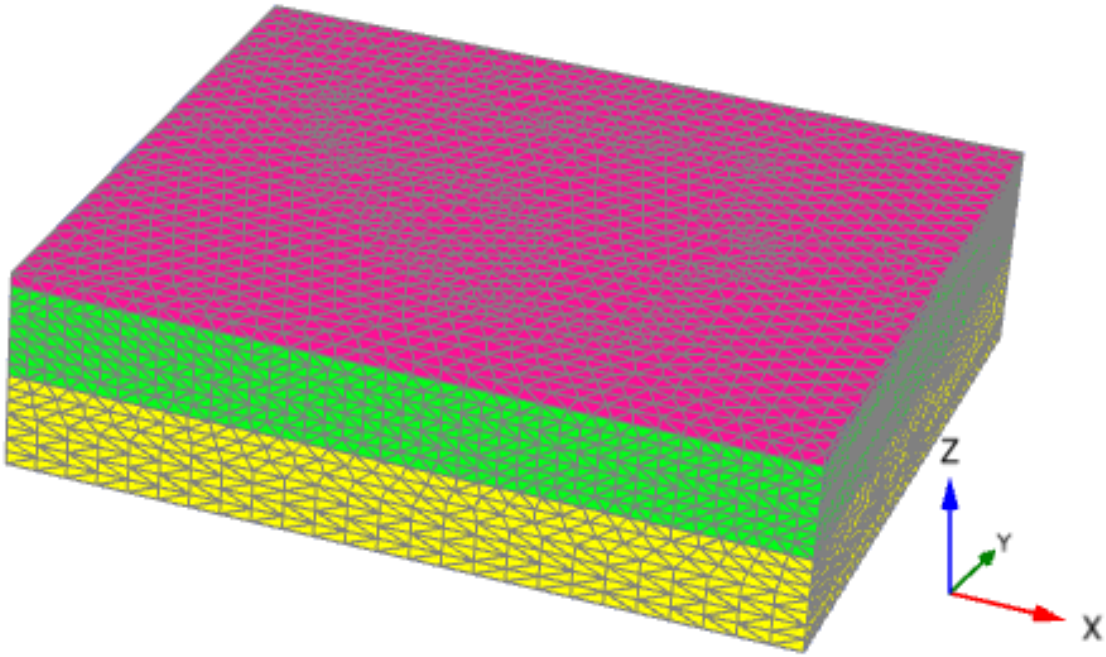

Figure 4.3 :- Mesh of Soil Layers

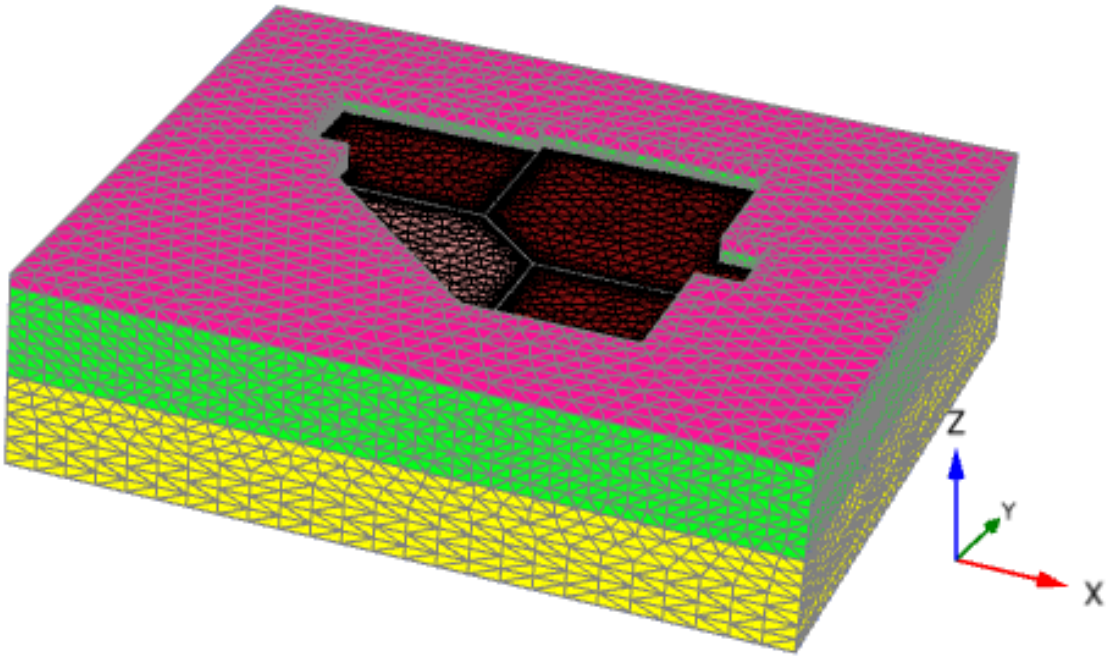

Figure 4.4 :- Mesh of Soil Layers after Load and Plate layout

4.7.4 Loading Condition

The structural analysis of each building block was done on **ETABS 2020** and the column loads from each were taken as point loads and applied on the soil as mentioned in **Appendix - B** . The rafts are considered as a plate element at the depth of 4m. the loads were applied at different times as all blocks were not constructed in same time i.e. Block D was constructed much later than other blocks.

Table 4.8 :- Material Properties of Raft

Parameter	**Symbol**	**Plate**	**Unit**
Property	-	Linear Elastic	-
Unit Weight	ϒ	25	kN/m^3
Modulus of Elasticity	E	$30*10^6$	kN/m^2
Thickness	D	1 (Block A, B and C) 0.91 (Block D)	m

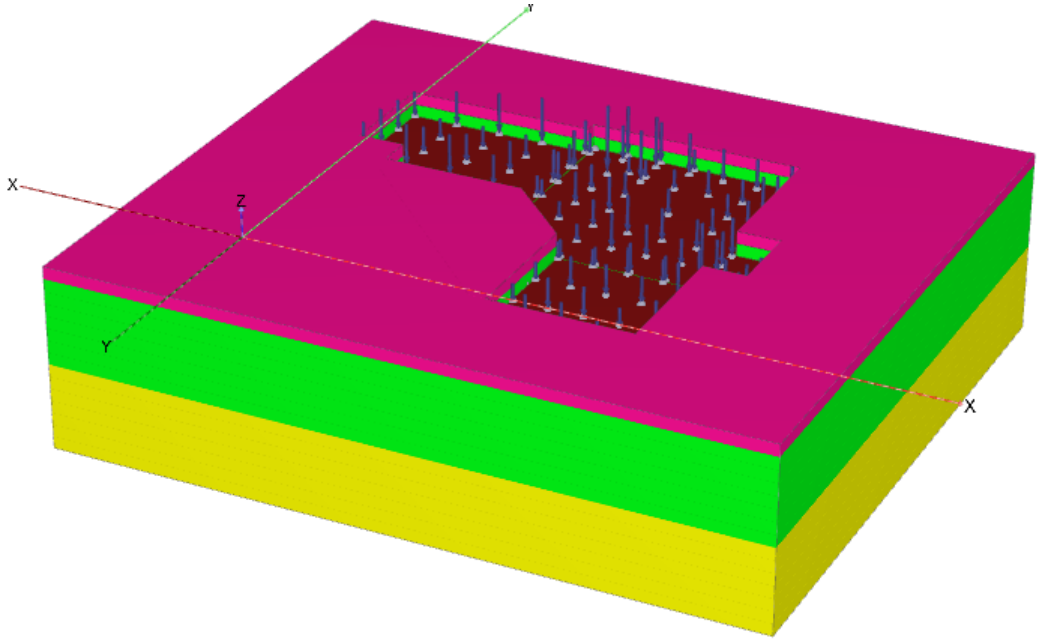

Figure 4.5 :- Soil layer after application of column load of Block A, B and C (Phase 1)

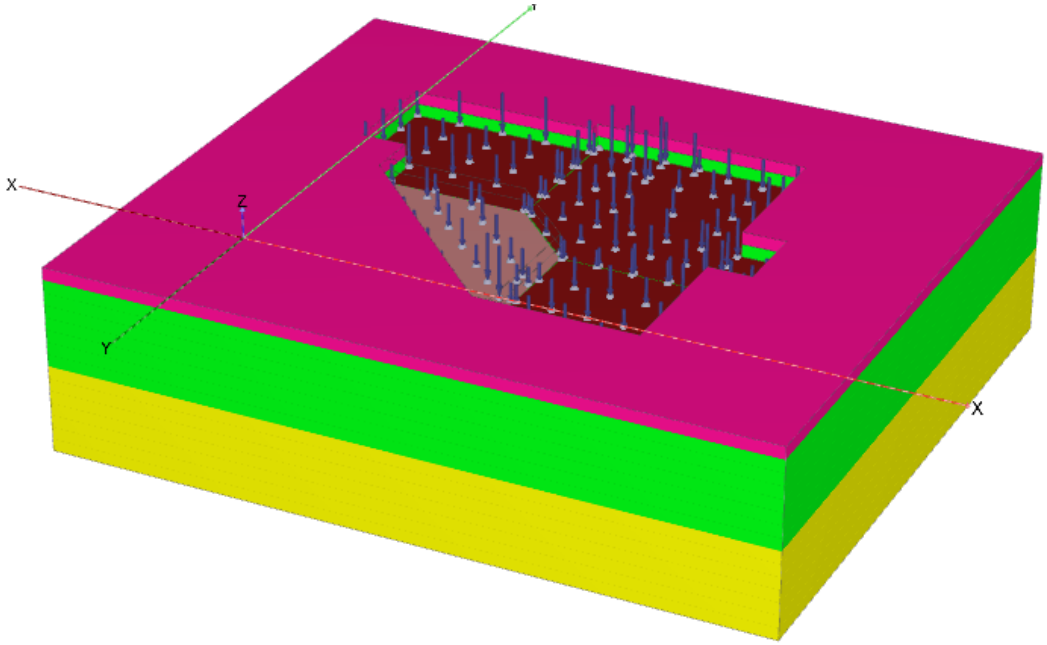

Figure 4.6 :- Soil layer after application of column load of Block A, B, C and D (Phase 2)

5 RESULT AND DISCUSSION

5.1 Introduction

In this chapter, the results of the settlement records will be presented and analyzed. The findings of this research mainly focused on two aspects. The first is the prediction of settlement based on Terzaghi's method, particularly that of numerical modelling. And the last one is the verification of result and behavior of time vs. settlement curve that was obtained from previous sample analysis and recent sample analysis. The discussion includes the evaluation of accuracy and limitations of these methods as they are compared with the settlement records.

Prior to presenting the main findings, an analysis of the allowable bearing capacity of the building based on the criteria of a maximum settlement is presented at the very beginning. Comparison between the building load and allowable bearing capacity would give light to trend of settlement displayed in building.

5.2 Consolidation

The method used to calculate the primary consolidation settlement has been described in Section 4.4. in Equation 4.2 was used to determine the consolidation settlement and (e, Log σ_v) plots was used to determine the change in void ratio for the corresponding change in stress. The calculation is presented in tabular form in Table 5.1. The primary consolidation settlement is estimated to be 179.30 mm from **Appendix - C** . Where the stress change is calculated from 2:1 stress distribution method. This value is considerably higher than the limit of maximum settlement described by IS 1904-2021, where 125 mm maximum settlement is stipulated for raft foundation on plastic clay soil. The fact that the estimated maximum settlement is much higher than the codal provision of 125 mm resulted from an appreciably higher load imposed on the soil, which is determined from **ETABS-Analysis** and shown detailly in **Appendix - B** . Even though the total settlement exceeds the limit, the angle distortion of building is within the limit of 1/300 IS 1904-2021 of suggesting the structural integrity.

Table 5.1 :- Calculation of Primary Consolidation Settlement

Layer Thickness 1m Water Table 0.6m

Unit weight of Water (Υ_w) 9.81 kN/m^3 Total Increase in Stress on Ground Surface 107.866 kN/m^2

Sub layer (m)	Mid height from Footing (m)	Mid height from Ground Surface (m)	Water Content (w)	Specific Gravity (Gs)	Bulk Unit Density (g/cm^3)	Bulk Unit Weight (kN/m^3)	Initial Void Ratio	Liquid Limit	Cc	σ_o' (kN/m^2)	l+z (m)	b+z (m)	$\Delta\sigma$= Q/A (kN/m^2)	Final Settlement (Sf) (m)
4-5	0.5	5.5	29.45	2.45	2.01	19.72	0.76	36.75	0.15	60.38	67	60	28.09	0.01416
5-6	1.5	6.5	29.45	2.45	2.01	19.72	0.75	36.75	0.15	70.29	69	62	26.39	0.01186
6-7	2.5	7.5	29.45	2.45	2.01	19.72	0.75	36.75	0.15	80.20	71	64	24.85	0.01007
7-8	3.5	8.5	29.45	2.45	2.01	19.72	0.74	36.75	0.15	90.10	73	66	23.43	0.00866
8-9	4.5	9.5	29.45	2.45	2.01	19.72	0.73	36.75	0.15	100.01	75	68	22.14	0.00751
9-10	5.5	10.5	36.33	2.61	1.9	18.64	0.73	39.5	0.15	108.84	77	70	20.95	0.00663
10-11	6.5	11.5	36.33	2.61	1.9	18.64	0.73	39.5	0.15	117.67	79	72	19.85	0.00589
11-12	7.5	12.5	23.02	2.65	2.01	19.72	0.72	38	0.15	127.58	81	74	18.84	0.00521
12-13	8.5	13.5	23.02	2.65	2.01	19.72	0.72	38	0.35	137.49	83	76	17.90	0.01084
13-14	9.5	14.5	23.02	2.65	2.01	19.72	0.71	38	0.35	147.40	85	78	17.03	0.00971
14-15	10.5	15.5	22.17	2.78	2.03	19.91	0.71	42.8	0.35	157.50	87	80	16.22	0.00872
15-16	11.5	16.5	22.17	2.78	2.03	19.91	0.70	42.8	0.35	167.60	89	82	15.47	0.00787
16-17	12.5	17.5	22.17	2.78	2.03	19.91	1.86	42.8	0.69	177.71	91	84	14.77	0.00837
17-18	13.5	18.5	22.17	2.78	2.03	19.91	1.85	42.8	0.69	187.81	93	86	14.12	0.00763
18-19	14.5	19.5	61.83	2.48	1.67	16.38	1.84	57	0.69	194.39	95	88	13.51	0.00709

Sub layer (m)	Mid height from Footing (m)	Mid height from Ground Surface (m)	Water Content (w)	Specific Gravity (Gs)	Bulk Unit Density (g/cm^3)	Bulk Unit Weight (kN/m^3)	Initial Void Ratio	Liquid Limit	Cc	σ_o' (kN/m^2)	l+z (m)	b+z (m)	$\Delta\sigma = Q/A$ (kN/m^2)	Final Settlement (Sf) (m)
19-20	15.5	20.5	61.83	2.48	1.67	16.38	1.83	57	0.69	200.96	97	90	12.93	0.00660
20-21	16.5	21.5	61.83	2.48	1.67	16.38	1.82	57	0.69	207.53	99	92	12.40	0.00616
21-22	17.5	22.5	61.83	2.48	1.67	16.38	1.82	57	0.69	214.10	101	94	11.89	0.00575
22-23	18.5	23.5	61.83	2.48	1.67	16.38	1.81	57	0.69	220.68	103	96	11.42	0.00538
23-24	19.5	24.5	61.83	2.48	1.67	16.38	1.80	57	0.69	227.25	105	98	10.97	0.00504
24-25	20.5	25.5	58.44	2.55	1.53	15.01	1.80	51.75	0.69	232.45	107	100	10.55	0.00476
25-26	21.5	26.5	58.44	2.55	1.53	15.01	1.79	51.75	0.69	237.65	109	102	10.15	0.00449
26-27	22.5	27.5	58.44	2.55	1.53	15.01	1.79	51.75	0.69	242.85	111	104	9.78	0.00425
27-28	23.5	28.5	58.44	2.55	1.53	15.01	1.78	51.75	0.69	248.05	113	106	9.43	0.00402
28-29	24.5	29.5	55.4	2.47	1.59	15.60	1.78	52	0.61	253.83	115	108	9.09	0.00336
29-30	25.5	30.5	55.4	2.47	1.59	15.60	1.77	52	0.61	259.62	117	110	8.77	0.00318
													Total Settlement (m)	0.18319
													Total Settlement (mm)	183.19

5.3 Settlement Analysis from PLAXIS-3D

For the prediction of settlement in this study we used the PLAXIS 3D. First of all, the geometry of the model has been prepared on PLAXIS 3D. The model taken for the calculation is shown in Figure 4.2. The geometrical model after the generation of the mesh is shown in Figure 4.3. After applying the point load throughout the foundation, the model was deformed uniformly as shown in Figure 5.1.

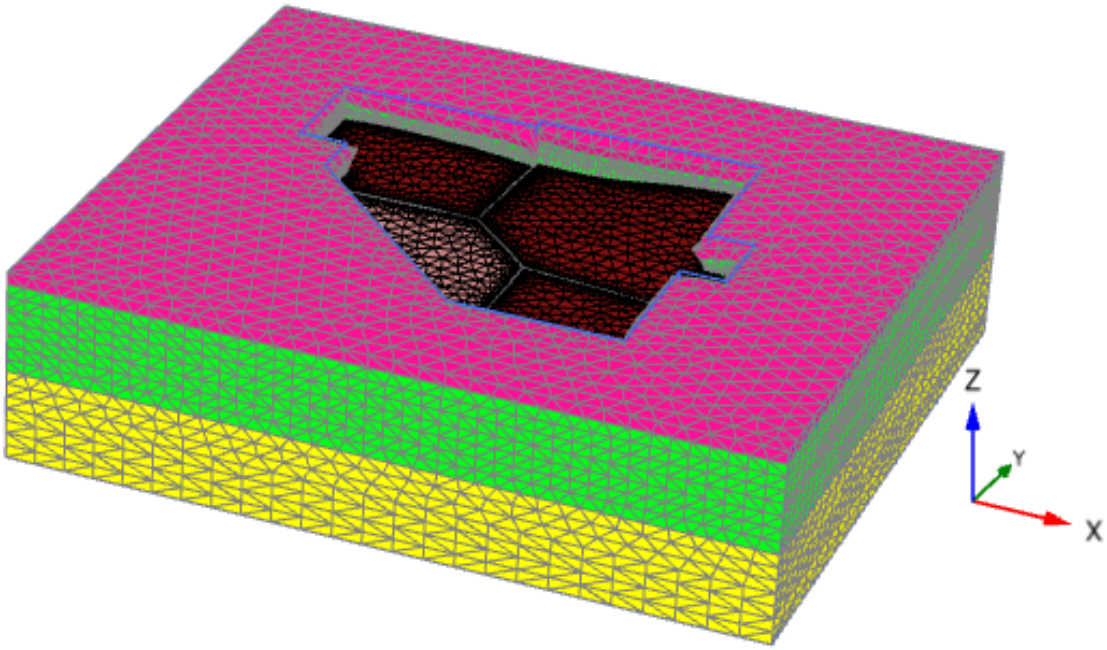

Figure 5.1 :-Deformed Mesh of Soil Layers after Load and Plate layout

5.3.1 Total Settlement

For the settlement analysis, models were built for separate borehole logs as per soil properties on Table 4.3, Table 4.4, Table 4.5, Table 4.6 and Table 4.7 for respective BH1, BH2, BH3, BH4 & BH5 and Table 4.8 for foundation or raft properties in PLAXIS-3D.

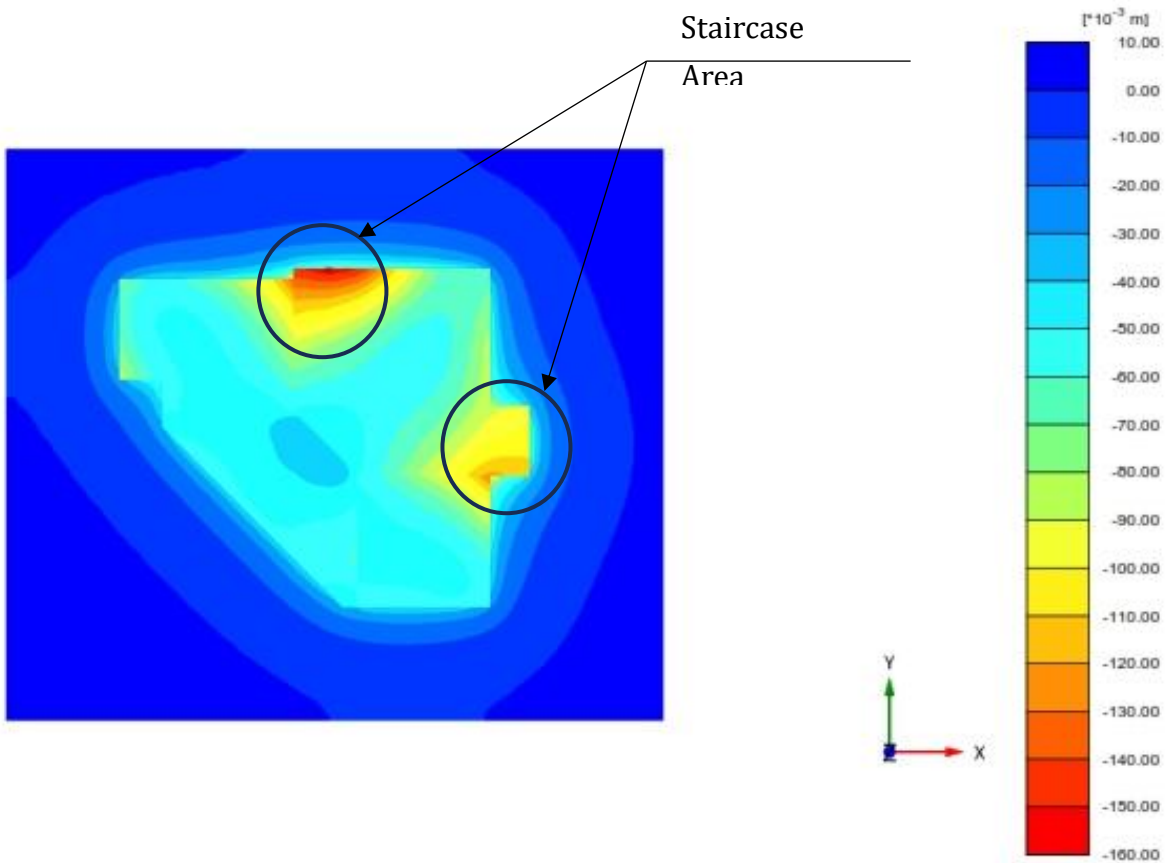

Figure 5.2 :- Building Settlement Contour Top view in BH-1

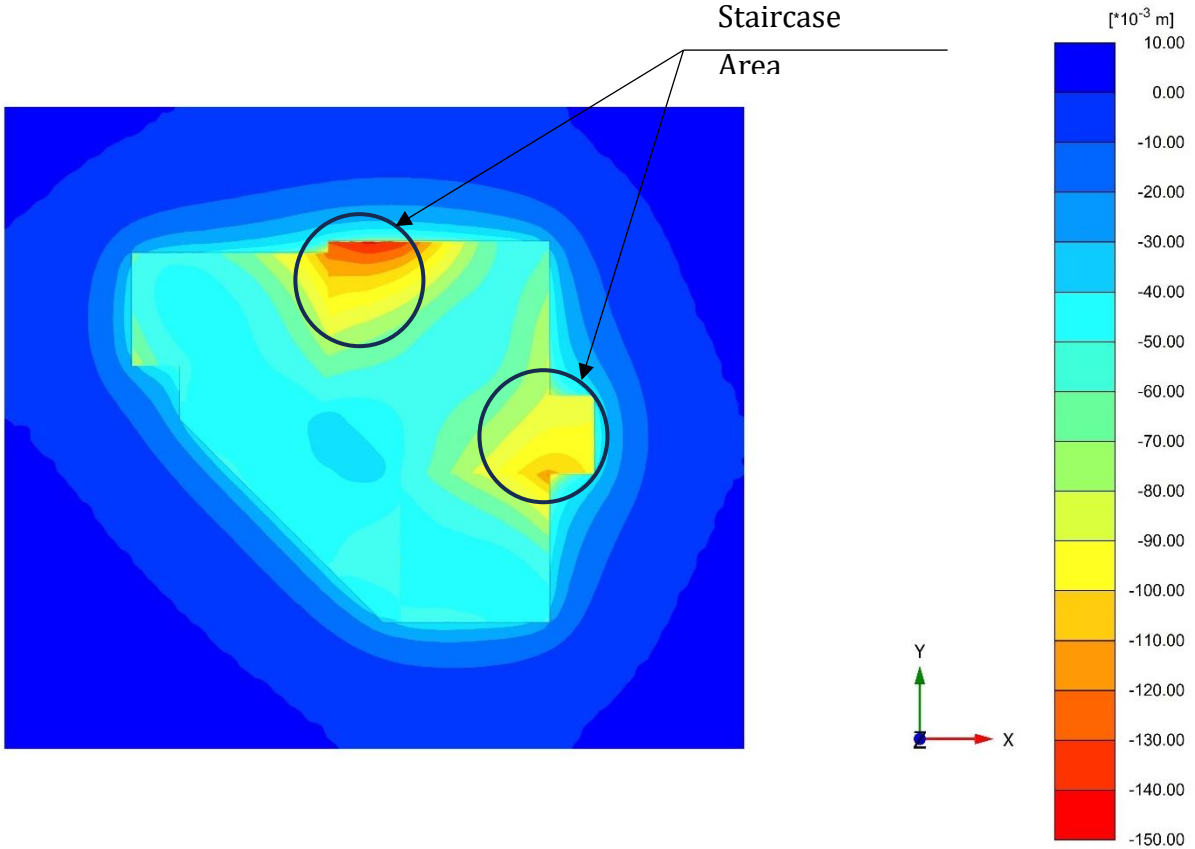

Figure 5.3 :- Building Settlement Contour Top view in BH-2

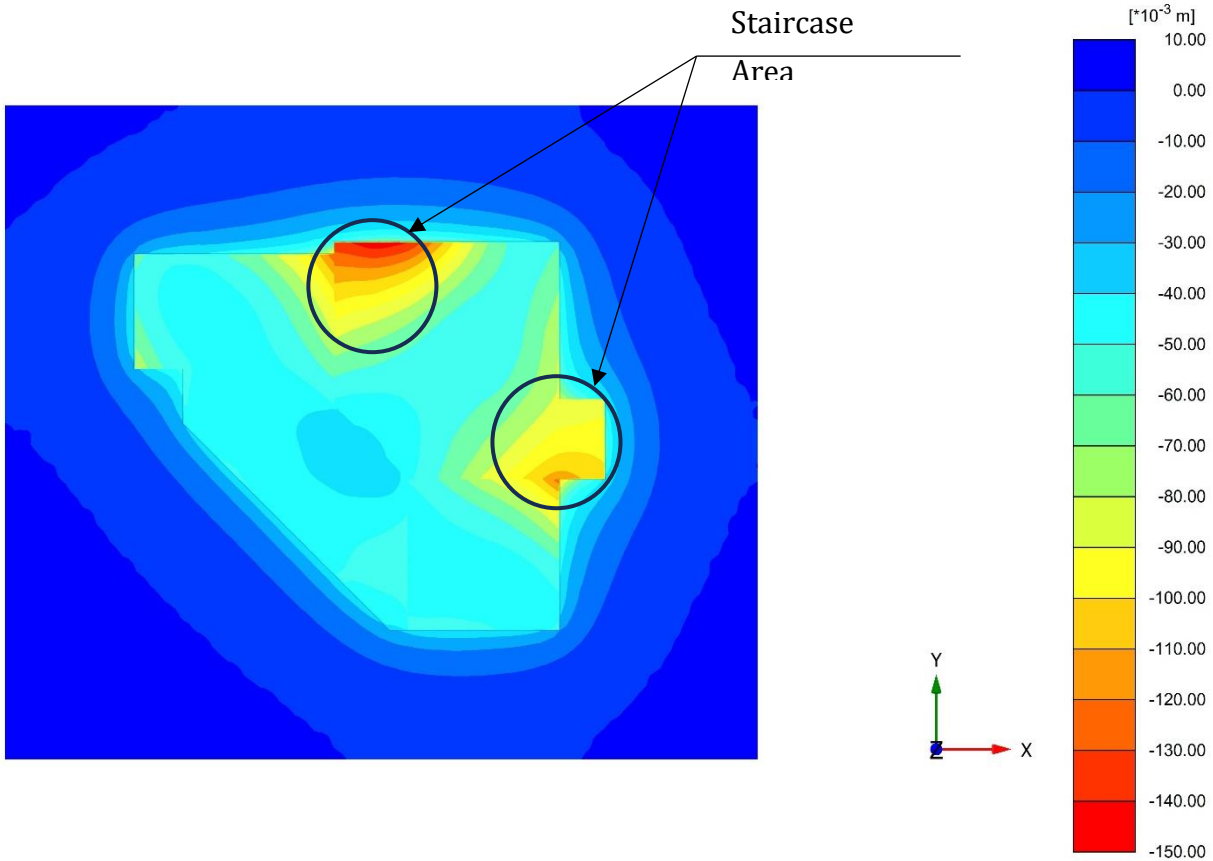

Figure 5.4 :- Building Settlement Contour Top view in BH-3

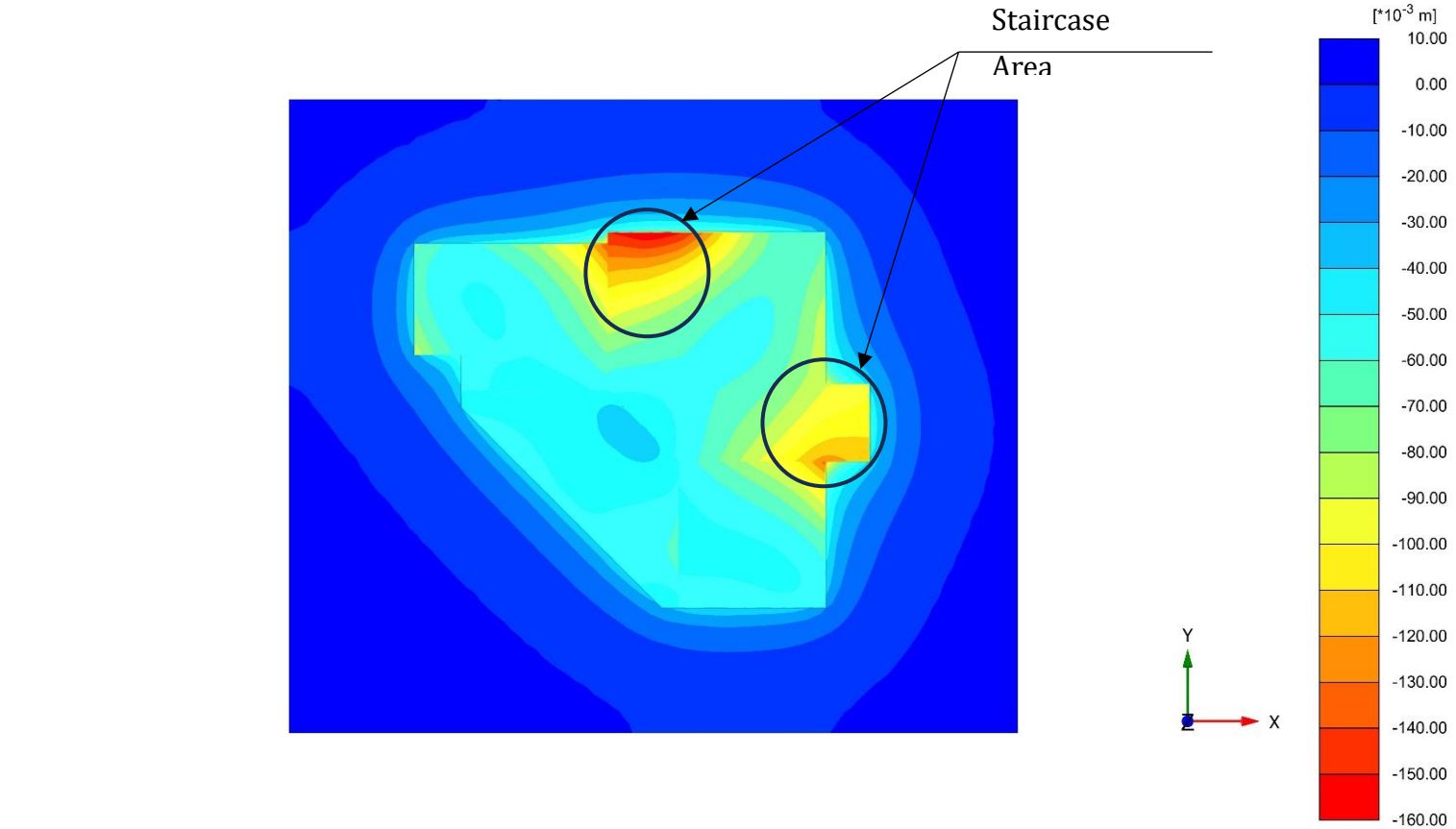

Figure 5.5 :- Building Settlement Contour Top view in BH-4

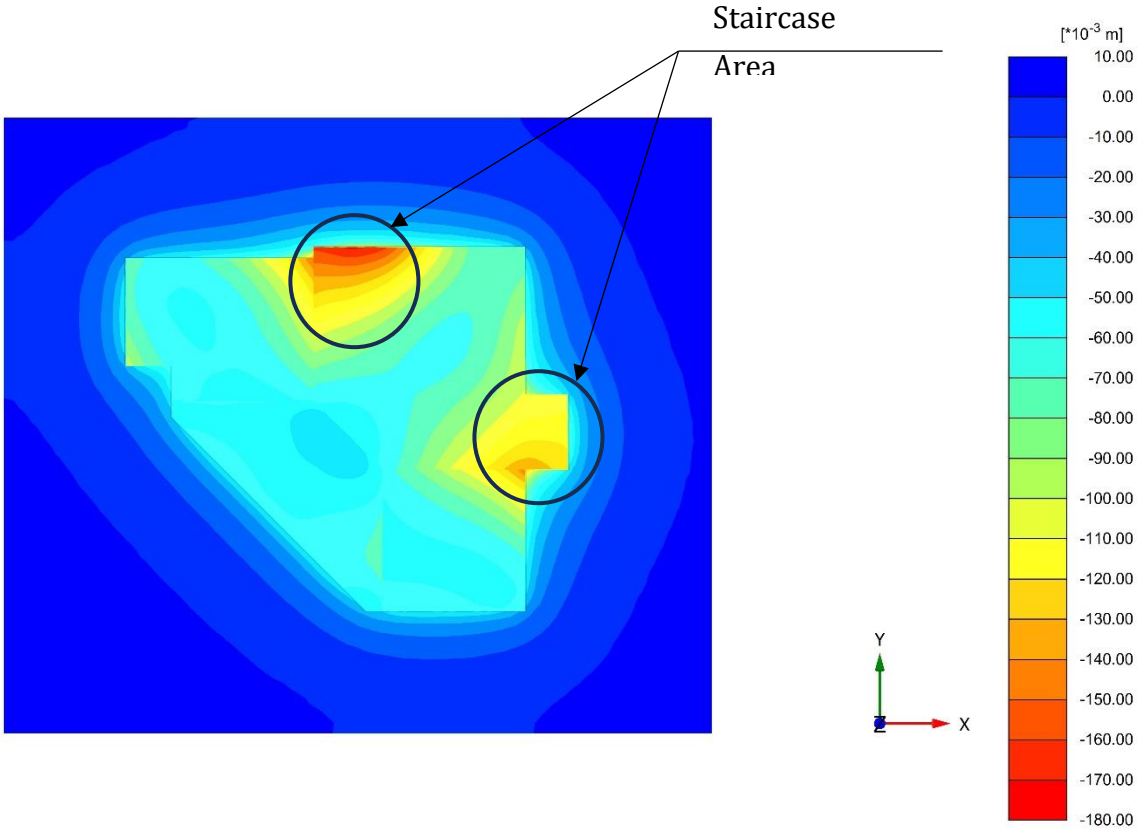

Total displacements u_z (scaled up 20.0 times) (Time 6740 day)

Maximum value = $2.311*10^{-3}$ m (Element 2992 at Node 6915)

Minimum value = -0.1726 m (Element 30012 at Node 5762)

Figure 5.6 :- Building Settlement Contour Top view in BH-5

The extreme total displacement for each borehole log is summarized in table below and was found to be average of 155.94 mm.

Table 5.2 :- Settlement Result from different Borehole

S.N.	Borehole	Excessive settlement (mm)
1	BH 1	157.9
2	BH 2	142.3
3	BH 3	147.1
4	BH 4	159.8
5	BH 5	172.6
	Average Settlement	**155.94**

The maximum settlement was observed at two locations in Block B within the raft foundation, specifically around the staircase areas. These zones carry a higher concentration of column loads compared to the rest of the foundation, as shown in the figure below. This occurs because staircases are typically supported by closely spaced or heavily loaded columns with higher live loads for commercial building, which transfer greater loads to the underlying soil.

In addition, the combined effect of higher imposed loads and dead loads, as presented in **Appendix - B**, further increases the stress intensity in these regions. When such concentrated loads act on compressible soil, they generate higher vertical stresses, leading to greater consolidation and settlement.

As a result, the raft foundation tends to undergo more pronounced deflection in these localized areas. This differential behavior is due to the staircase regions exhibiting higher settlement compared to the relatively uniformly loaded portions of the foundation.

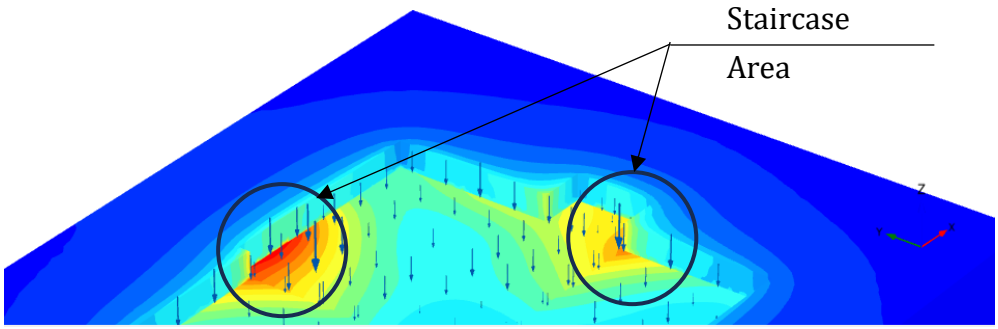

Figure 5.7 :- Load Concentration around Staircase Area

5.3.2 Differential Settlement

Differential settlement is generally more critical than total settlement because even small variations in settlement across a structure can lead to significant structural and serviceability issues. Uneven settlement induces internal stresses in structural elements, which may result in cracking of beams, slabs, and walls, as well as distortion of the structural frame. In addition, it can cause functional problems such as sloping floors, misalignment, and the jamming of doors and windows, thereby affecting the overall performance and usability of the structure.

So, the differential settlement was calculated as,

Min settlement (S_{min}) = 0.0407 m

Max settlement (S_{max}) = 0.1487 m

Length (L) = 37.5 m

Difference in settlement (ΔS) = S_{max} - S_{min} = 0.1487 – 0.0407

= 0.108 m

Angular Distortion (β) $= \frac{\Delta S}{L} = \frac{0.108}{37.5} = \frac{1}{347}$

The angular distortion calculated as per the section passing through high settlement area as shown in Figure 5.8 and was found to be around 1/347 which is lower than the 1/300 as per IS 1904-2021 for multi storied RC building in plastic clay.

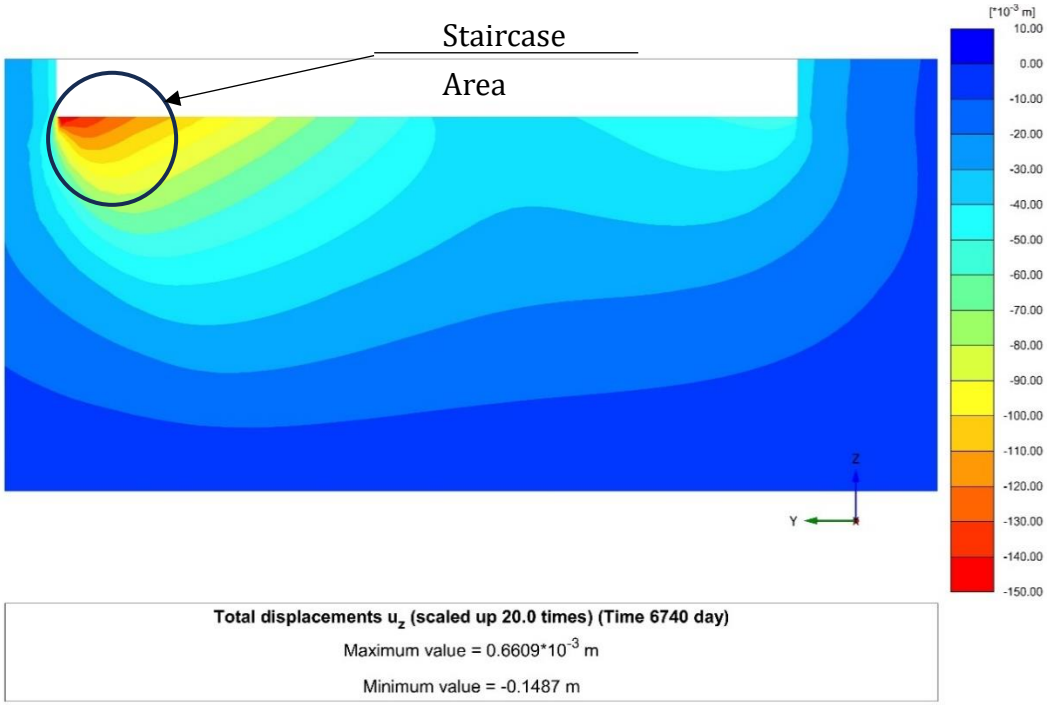

Figure 5.8 :- Section along X-axis passing through the high stress area at end of Phase-2

5.3.3 Construction Induced settlement

The settlement before and after construction of Phase 2 i.e. Block D is shown at max settlement places i.e. node 94 (Figure 5.9 and Figure 5.10) and node 194 (Figure 5.11 and Figure 5.12) and there has been negligible impact on settlement, due to construction of building Block D on surrounding settlement at Block A, B &C. It might be because the soil underlying Block A, B &C have already reached 83.829% as per Table C.1 **(Appendix - C)** of degree of consolidation during start of construction of Block D.

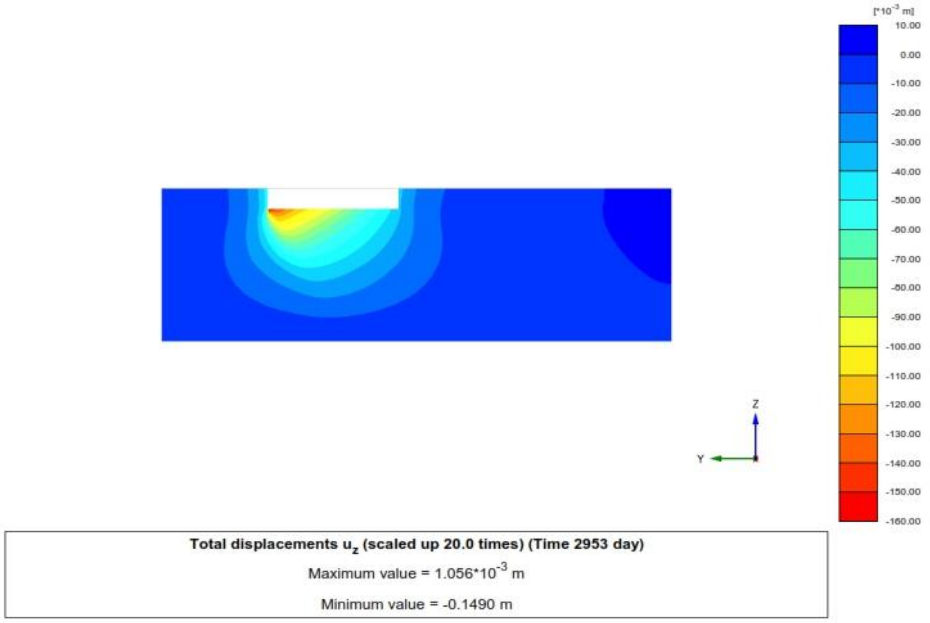

Figure 5.9 :- Building Settlement in section at along x-axis at BH-1 at the end of Phase 1 along Node 94

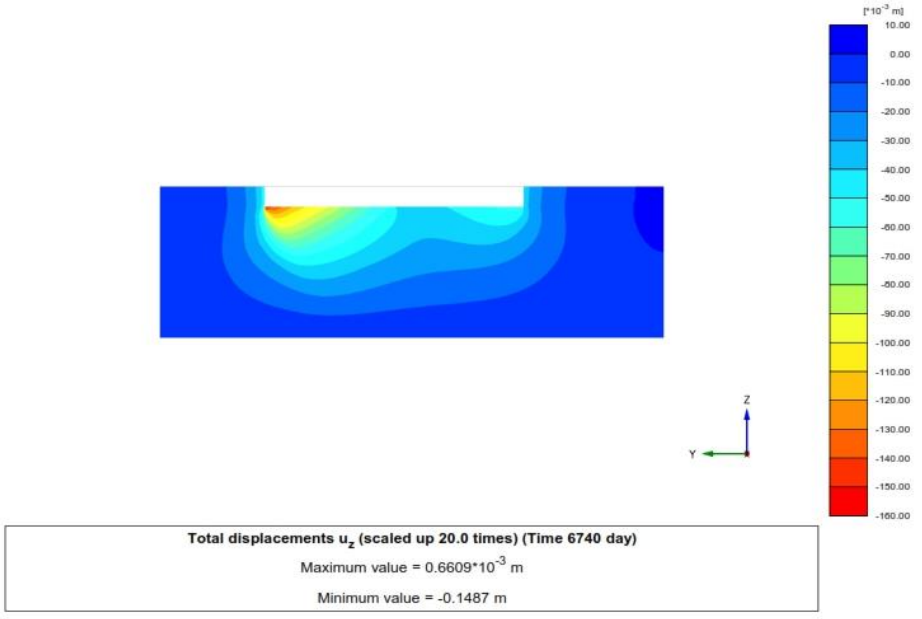

Figure 5.10 :- Building Settlement in section at along x-axis at BH-1 at the end of Phase 2 along Node 94

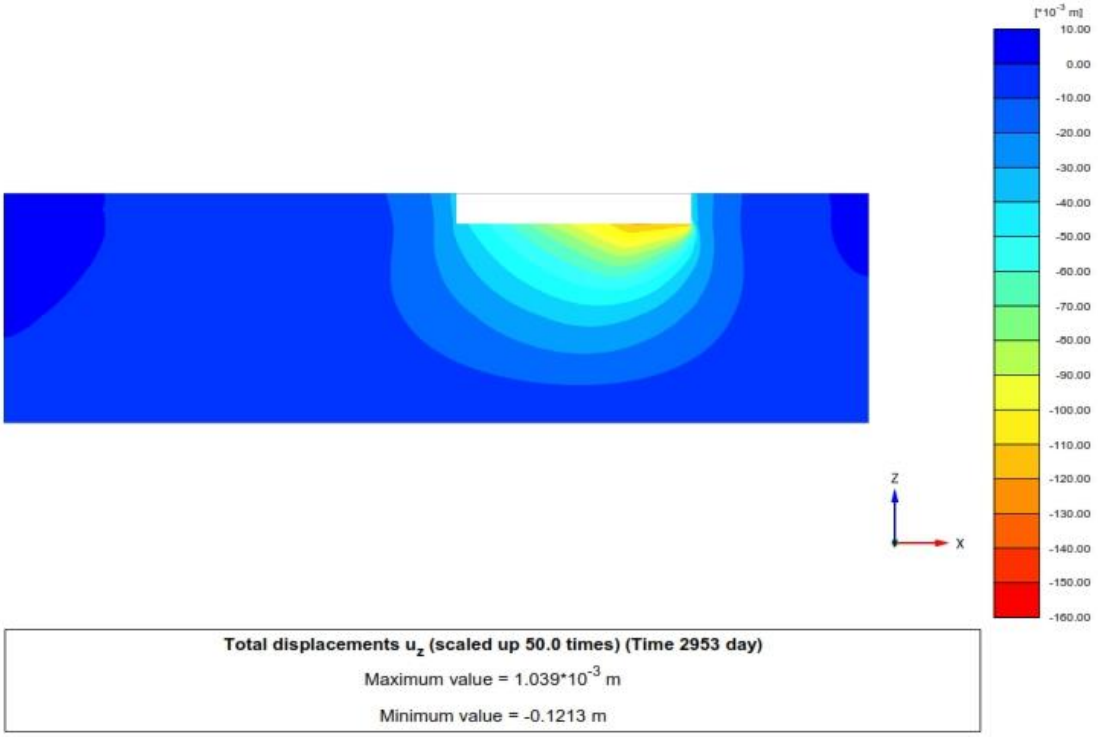

Figure 5.11 :- Building Settlement in section at along y-axis at BH-1 at the end of Phase 1 along Node 194

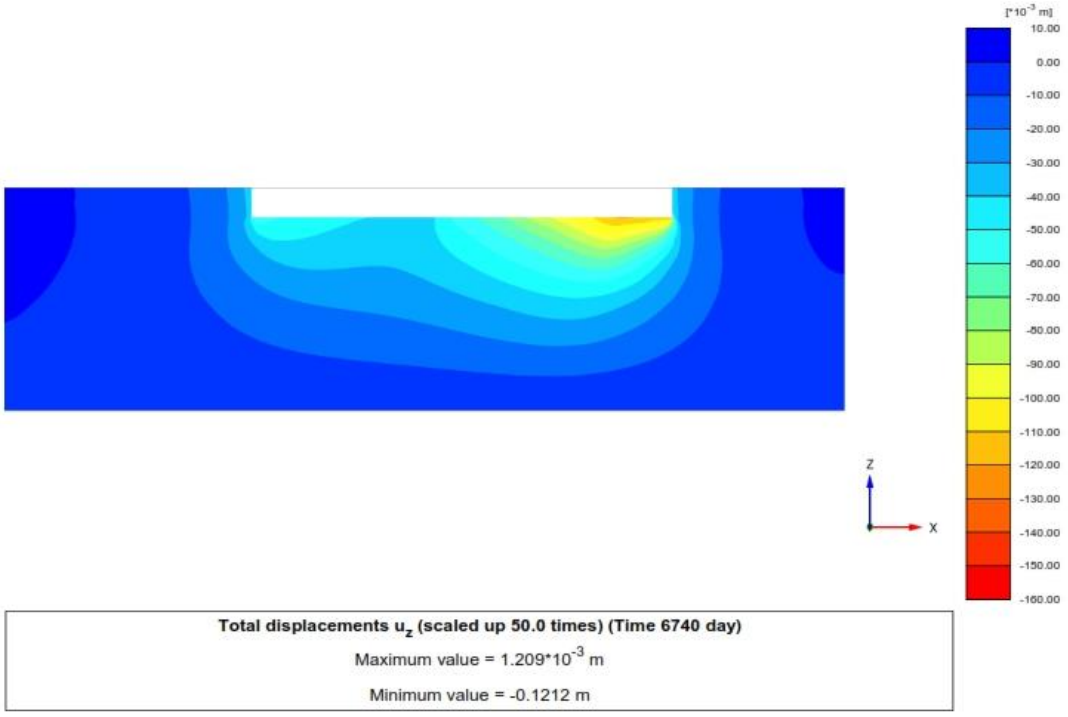

Figure 5.12 :- Building Settlement in section at along y-axis at BH-1 at the end of Phase 2 along Node 194

5.4 Settlement Calculation by Janbu Method

From Eq. 2.13 we have,

$$S_e = A_1 A_2 \frac{q_0 B}{E_s}$$

As depth of rigid layer is unknown i.e., H = ∞

$A_1 = 0.9$

Width of Foundation (B) = 59 m

Depth of Foundation (D_f) = 4 m

Then, D_f / B = 0.068

So from Figure 2.4, we have $A_2 = 0.98$

We have,

Stress on Soil (q_0) = 107.866 kN/m^2

Modulus of Elasticity (E_s) = 31880 kN/m^3

Total settlement (S_e) = 176.071 mm

For, Degree of Consolidation (U) = 97.875 % (From **Appendix - C**)

Current Settlement (S_f) = 172.329 mm

5.5 Comparison of Settlement

Block A, B and C were constructed and in second phase Block D was constructed. Construction of first phase building Block A, B and C started in 2007 March and of second phase building Block D started in 2015 April. So, the time period for Phase 1 is taken as 2,953 days and Phase 2 is taken as 3,787 days totaling 6,740 days.

Terzaghi's method of settlement determination technique was carried out for building in **Appendix - C** and Table 5.1. The determined value is then compared with the observation results. Also, the result was compared with numerical modelling PLAXIS 3D. The comparison of result is determined from two different approach **(Terzaghi and Janbu Method of Settlement Analysis)** is shown in Table 5.3.

Table 5.3 :- Settlement Comparison

Parameter	From Plaxis-3D	From Terzaghi	From Janbu
Settlement (mm)	155.94	179.297	172.329

6 CONCLUSION AND RECOMMENDATION

6.1 Conclusion

From the settlement prediction analysis and from the numerical modelling, the following conclusions can be drawn.

- Soil stratigraphy analysis confirmed a highly compressible profile, with medium-stiff grey silty soil (0–16 m) underlain by stiff organic clay (16–30 m), both exhibiting low permeability and high compressibility, making the site highly susceptible to consolidation settlement.
- Analytical settlement estimation using Terzaghi's 1-D consolidation theory and layer-wise stress increment calculations (2:1 method) yielded a total primary consolidation settlement of 179.30 mm.
- Consolidation parameters obtained from laboratory data (void ratio–log σ′ curves, compression index C_c, and coefficient of consolidation C_v via square-root–time method) indicated that the soil layers beneath the foundation have undergone approximately 97–98% primary consolidation, signifying approach toward the secondary compression phase.
- Numerical modelling using PLAXIS 3D, incorporating actual stratigraphy, Mohr–Coulomb constitutive behavior, staged construction (Phase 1: Blocks A–C; Phase 2: Block D), and realistic boundary conditions, predicted an average total settlement of 155.94 mm across five boreholes.
- Empirical settlement analysis from Janbu method has estimated the settlement of 172.329 mm.
- Comparison between analytical, numerical and empirical results exhibited strong agreement, with PLAXIS results being approximately 13% lower of Terzaghi and 9.5% lower of Janbu method, attributable to 3D stress redistribution and non-linear interaction effects captured by FEM but neglected in 1D theory.
- The maximum angle distortion of building is 1/347 and lies within the permissible limit of 1/300 as set by IS 1904-2021 for multi storied RC buildings in plastic clay.
- Settlement assessment demonstrated no additional deformation between construction phases, indicating that the addition of Block D did not produce significant stress overlap or interaction with Blocks A–C.
- Stress redistribution visualized in PLAXIS showed uniform settlement, affirming that the raft foundation provides adequate load distribution across

variable soil stiffness zones, with critical localized deformation around Staircase which have higher load concentration than other areas.

- The combined results conclusively show that majority of settlement has already occurred, and future long-term deformation will be governed mainly by secondary consolidation of the deep organic clay layer.

6.2 Limitation

- Absence of field settlement monitoring data prevented validation of analytical and numerical predictions using actual observed settlement profiles.
- Soil data were available only up to 30 m depth, requiring the assumption that compressible layers below this depth would not significantly influence long-term settlement.
- Groundwater level was assumed constant throughout the analysis, whereas seasonal fluctuations and long-term groundwater decline in Kathmandu Valley may alter effective stress and consolidation behavior.
- Changes in structural loading after construction, such as renovation, additional service loads, or occupancy variations, were not incorporated into the analysis.
- Influence of seismic loading and earthquake-triggered reconsolidation settlement was not considered, despite Kathmandu's high seismicity and the potential for cyclic softening in lacustrine clays.
- Secondary compression behavior was not calibrated using site-specific long-term data, and creep parameters were inferred indirectly rather than measured through long-duration oedometer testing.
- Interaction effects between adjacent structures and regional subsidence in Lalitpur were not included, though both may influence long-term settlement trends.

REFERENCES

Al-Taie, E., Al-Ansari, N., & Knutsson, S. (2016). *Evaluation of foundation settlement under various added loads in different locations of Iraq using finite element*. Engineering*, 8*(5), 257–268.

Bezih, K., Chateauneuf, A., & Demagh, R. (2020). *Effect of long-term soil deformations on RC structures including soil–structure interaction*. Civil Engineering Journal, 6(12), 2290–2310

Bhattarai, R., Alifu, H., Maitiniyazi, A., & Kondoh, A. (2017). Detection of land subsidence in Kathmandu Valley, Nepal, using DInSAR technique. *Land, 6*(2), 39

Bhutto, A. H., Bhurgri, G. S., Zardari, S., Zardari, M. A., Memon, B. A., & Babar, M. M. (2020). Settlement response of a multi-story building. *Engineering, Technology & Applied Science Research*, 10(5), 6220–6223

Bowles, J. E. (1996). *Foundation Analysis and Design*. McGraw-Hill.

Christian, J. T., & Carrier III, W. D. (1978). Janbu, Bjerrum and Kjaernsli's chart reinterpreted. *Canadian Geotechnical Journal, 15*(1), 123–128.

CMTL (2002) *Final report on soil investigations work for Lalitpur Bishal Bazar Complex, Pulchowk , Lalitpur*.

Das, B. M. (2016). *Principles of foundation engineering* (8e ed.). Cengage

Devkota, P. (2018). *Settlement observation and analysis of ICT Pulchowk*

E. S. Barber. *Notes on Secondary Consolidation*, 1961.

Fox, E. N. (1948*). The mean elastic settlement of flexible foundations*. Proceedings of the Second International Conference on Soil Mechanics and Foundation Engineering, 2, 129–132.

G. Mesri, and T. Feng. *Consolidation of Soils*, 2014.

Janbu, N., Bjerrum, L., & Kjaernsli, B. (1956). *Veiledning ved løsning av fundamenteringsoppgaver*. Norwegian Geotechnical Institute.

Lambe, T. W., & Whitman, R. V. (1969). *Soil Mechanics*. John Wiley & Sons.

M. Al-Zoubi. *Consolidation Analysis by the Slope and Settlement Rate - Settlement Methods*, 2013.

Mesri, G., & Castro, A. (1987). *Cα/Cc Concept and K0 during Secondary Compression. Journal of Geotechnical Engineering*, 113(3), 230-247.

Neeru K. C., & Dahal, K. R. (2020). Investigation of soil at different locations of the Kathmandu Valley of Nepal. *American Journal of Science, Engineering and Technology, 5*(4), 154–169.

Nguyen, T., Tran, Q., & Pham, H. (2018). *Numerical Model Validation for Commercial Complex Settlement Analysis.* Journal of Civil Engineering and Management, 24(1), 31-42.

Patrício, J. D., Gusmão, A. D., Ferreira, S. R. M., Silva, F. A. N., Kafshgarkolaei, H. J., Azevedo, A. C., & Delgado, J. M. P. Q. (2024). *Settlement analysis of concrete-walled buildings using soil–structure interactions and finite element modeling*. Buildings, 14(3), 746

Paudel, M. R., & Sakai, H. (2008). *Stratigraphy and depositional environments of basin-fill sediments in southern Kathmandu Valley, Central Nepal*. Bulletin of the Department of Geology, Tribhuvan University, 11, 61–70

Poulos, H. G., & Davis, E. H. (2011). *Elastic Solutions for Soil and Rock Mechanics*. Springer

Raheena, M., & Robinson, R. G. (2020). *Determination of coefficient of secondary compression in accelerated incremental loading consolidation test*. In Geotechnical Investigations and Modelling: Proceedings of IGC 2018.

Robinson, R. G. (2003). A study on the beginning of secondary compression of soils. *Journal of Testing and Evaluation*.

S. Handali & S. Maharjan (2020) *Settlement of A Six-Story Building on A Soft Organic Clay Deposit in Kathmandu, Nepal*. Civil Engineering, Environmental and Disaster Risk Management Symposium

Shrestha, S., & Bajracharya, S. B. (2023). *Analyzing circulation efficiency in commercial complexes: A post-occupancy evaluation study in Kathmandu*. In Proceedings of the 14th IOE Graduate Conference. IOE, Tribhuvan University

Steinbrenner, W. (1934). *Tables for Settlement Calculation. Die Bautechnik*, 12, 256–258.

T. Tan. *Secondary Time Effects and Consolidation of Clays*, 1958.

Terzaghi, K. (1943). *Theoretical Soil Mechanics*. Wiley.

Terzaghi, K., Peck, R. B., & Mesri, G. (1996). *Soil Mechanics in Engineering Practice*. John Wiley & Sons.

Tewatia, S. K. (2013). *Trend of settlement in primary and secondary consolidations*. Geomechanics and Geoengineering, *8*(2), 125–134

Tiwari, B., Ajmera, B., & Timbadia, V. (2019). *Case Study—Settlement of a Hydropower Dam Structure during the 2015 Gorkha Earthquake.* In *Geo-Congress 2019: Embankments, Dams, and Slopes* (Geotechnical Special Publication 305, pp. 258–266). American Society of Civil Engineers.

Quintero, J., Millen, M., & Viana da Fonseca, A. (2024). *Sensitivity analysis of the effects of liquefiable soil deposits on differential settlement of buildings by numerical modelling*. In *Geotechnical Engineering Challenges to Meet Current and Emerging Needs of Society* (Vol. 18, pp. ...). Taylor & Francis.

APPENDIX - A BOREHOLE LOG

Table A.1 :- Soil profile of Borehole Log 1 in Labim Mall

Borehole Log
Borehole 1

Location: Pulchowk, Laitpur
Toatal Depth: 30 m
GWT: 0.6 m

Layer	Sample	ϒ (gm/cm^3)	Depth (m)	w %	SPT N value
Top Soil with fill Material and vegetation			0		
Dark Grey soft to medium stiff **Silt** of low plasticity (**ML**)	DS1	1.99		31.02	4
	DS2	1.98	2	31.96	2
	DS3	2.01	4	29.45	3
	DS4	1.89	6	31.58	3
	UD1				
	DS5	1.87		33.2	4
	DS6	1.9	8	36.33	5
	DS7	2.01	10	23.02	8
	UD2				
	DS8	1.69	12	45.84	6
	DS9	2.03		22.17	6
	DS10	1.95	14	30.7	8
Dark Grey stiff organic **Clay** of high plasticity (**OH**)	DS11	1.52	16	70.2	9
	UD3				
	DS12	1.67	18	61.83	9
	DS13	1.63		62.92	10
	DS14	1.63	20	52.85	9
	DS15	1.53	22	58.44	9
	DS16	1.48	24	95.45	-
	UD4				
	DS17	-		-	14
	DS18	-	26	-	14
	DS19	1.59	28	55.4	15
	DS20	1.5	30	89.43	15
End of Drilling at 30m					

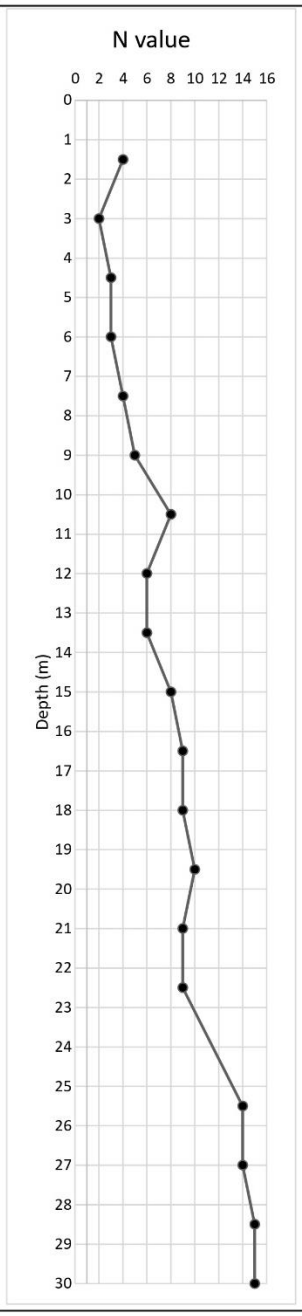

(Source: - *CMTL (2002)*)

Table A.2 :- Soil profile of Borehole Log 2 in Labim Mall

Borehole Log
Borehole 2

Location: Pulchowk, Laitpur
Toatal Depth: 30 m
GWT: 0.9 m

Layer	Sample	ϒ (gm/cm^3)	Depth (m)	w %	SPT N value	SPT Curve
Top Soil with fill Material and vegetation			0			
Grey to dark grey medium stiff to stiff **Silt** of low plasticity (**ML**)	DS1	1.82		30.4	9	
			2			
	DS2	1.92		28.11	8	
			4			
	DS3	1.94		27.81	9	
	DS4	1.98	6	27.53	7	
	DS5	1.96		29.62	10	
			8			
	DS6	1.95		28.01	9	
			10			
	DS7	1.83		32.6	9	
	DS8		12		-	
	UD1	1.88		47.22		
	DS9				10	
			14			
	DS10	1.81		33.36	11	
			16			
Dark Grey stiff organic **Clay** of high plasticity (**OH**)	DS11	1.61		55.31	11	
	DS12	1.47	18	78.8	-	
	UD2					
	DS13	1.63		56.15	7	
			20			
	DS14	1.62		63.03	9	
		1.37	22			
	DS15			69.24	11	
	DS16	1.36	24	122.76	10	
	DS17				-	
			26			
	DS18	1.48		82.92	10	
			28			
	DS19	1.4		98.94	9	
	DS20	1.46	30	103.43	10	
End of Drilling at 30m						

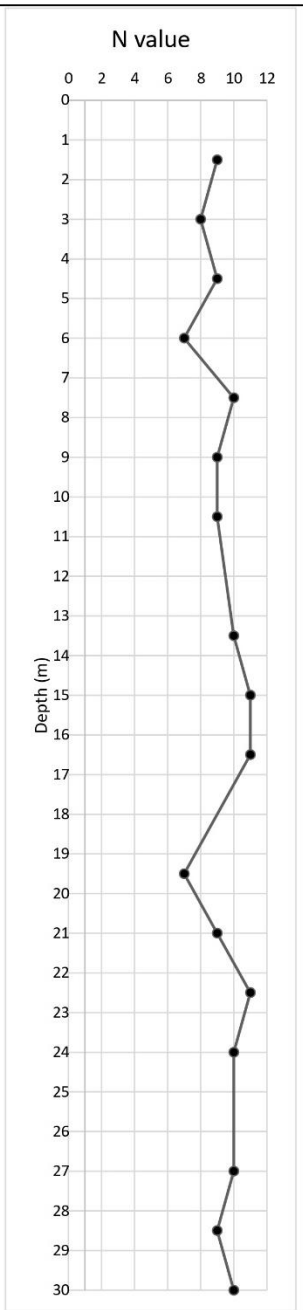

(Source: - *CMTL (2002)*)

Table A.3 :- Soil profile of Borehole Log 3 in Labim Mall

Borehole Log
Borehole 3

Location: Pulchowk, Laitpur
Toatal Depth: 30 m
GWT: 0.95 m

Layer	Sample	ϒ (gm/cm^3)	Depth (m)	w %	SPT N value	SPT Curve
Top Soil with fill Material and vegetation			0			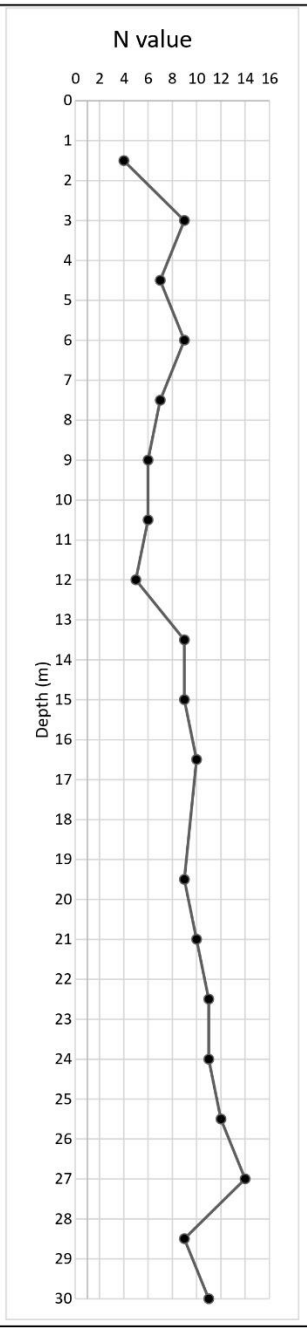
Grey to dark grey medium stiff to stiff **Silt** of low plasticity (**ML**)	DS1	2.21		27.2	4	
	DS2	2.17	2	26.86	9	
	DS3	1.91	4	26.42	7	
	DS4	-	6	-	9	
	DS5	1.98		28.36	7	
	DS6	2.17	8	31.27	6	
	DS7	1.88	10	26.12	6	
	UD1	1.89		47.17		
	DS8	1.82	12	45.73	5	
	DS9	1.82		45.73	9	
	DS10	1.78	14	52.19	9	
Dark Grey stiff organic **Clay** of high plasticity (**OH**)	DS11	2	16	44.89	10	
	DS12	1.6	18	56.79	-	
	UD2					
	DS13	1.92		35.92	9	
	DS14	1.69	20	77.38	10	
	DS15	1.88	22	32.52	11	
	DS16	-	24	-	11	
	UD3	1.54		95.26		
	DS17	1.68		66.42	12	
	DS18	1.41	26	103.8	14	
	DS19	1.71	28	70.43	9	
	DS20	1.55	30	83.44	11	
End of Drilling at 30m						

(Source: - *CMTL (2002)*)

Table A.4 :- Soil profile of Borehole Log 4 in Labim Mall

Borehole Log
Borehole 4

Location: Pulchowk, Laitpur
Toatal Depth: 30 m
GWT: 0.6 m

Layer	Sample	Υ (gm/cm^3)	Depth (m)	w %	SPT N value
Top Soil with fill Material and vegetation			0		
Grey to dark grey medium stiff **Silt** of low plasticity (**ML**)	DS1	2.13		29.04	-
	DS2	1.92	2	31.46	4
	DS3	1.94	4	29.2	3
	DS4	1.83	6	30.35	6
	DS5	2.05		32.41	5
	DS6	1.89	8	32.3	8
	DS7	1.96	10	30.13	7
	DS8	2.05	12	34.07	7
	DS9	1.64		62.1	6
	DS10	1.82	14	54.37	7
	DS11	1.91	16	30.93	7
Dark Grey stiff organic **Clay** of high plasticity (**OH**)	DS12	1.68	18	110.73	-
	UD1				
	DS13	1.63		59.8	7
	DS14	-	20	-	8
	DS15	-	22	-	9
	DS16	-	24	-	9
	DS17	-		-	-
	UD2	1.51	26	115.6	
	DS18	1.49		83.47	12
	DS19	1.45	28	72.82	13
	DS20	1.36	30	90.09	13
End of Drilling at 30m					

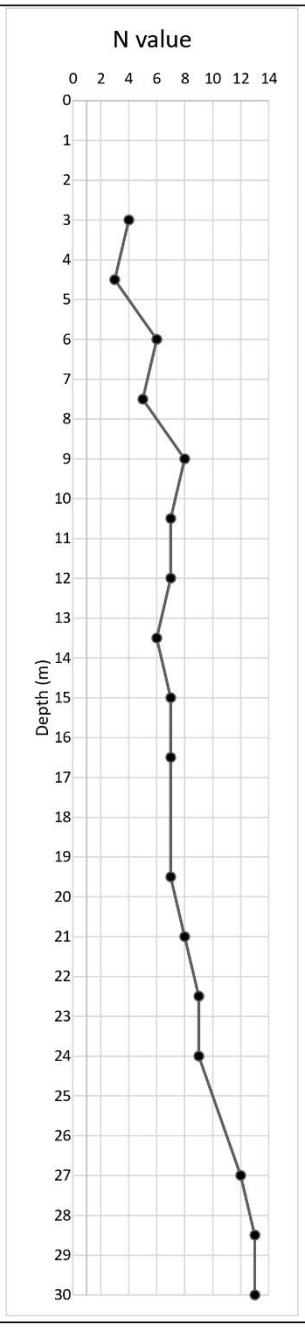

(Source: - *CMTL (2002)*)

Table A.5 :- Soil profile of Borehole Log 5 in Labim Mall

Borehole Log
Borehole 5

Location: Pulchowk, Laitpur
Toatal Depth: 30 m
GWT: 0.32 m

Layer	Sample	ϒ (gm/cm^3)	Depth (m)	w %	SPT N value
Top Soil with fill Material and vegetation			0		
Dark Grey soft to medium stiff **Silt** of low plasticity (**ML**)	DS1	2.13		30.58	3
	DS2	1.79	2	22.35	3
	DS3	2	4	32.5	2
	DS4	1.96	6	34.26	3
	UD1				
	DS5	1.95		43.4	5
	DS6	2.05	8	31.67	6
	DS7	1.96	10	30.13	6
	DS8	1.98	12	31.99	7
	DS9	2.1		29	8
	DS10	1.55	14	67	7
Dark Grey stiff organic **Clay** of high plasticity (**OH**)	DS11	1.56	16	67.83	-
	UD2				
	DS12	1.56	18	62	8
	DS13	1.54		80.5	9
	DS14	1.58	20	92.69	10
	DS15	1.44	22	93.71	10
	DS16	1.5	24	113.09	11
	DS17	1.58		82.46	11
	UD3		26		
	DS18	1.65		96.72	10
	DS19	1.45	28	94.37	11
	DS20	1.42	30	105.54	11
End of Drilling at 30m					

SPT Curve

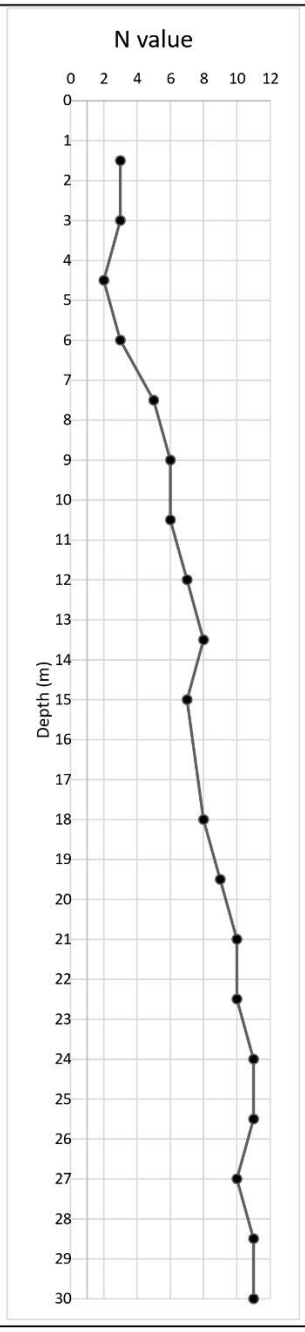

(Source: - *CMTL (2002)*)

APPENDIX - B LOAD CALCULATION

ETABS Analysis

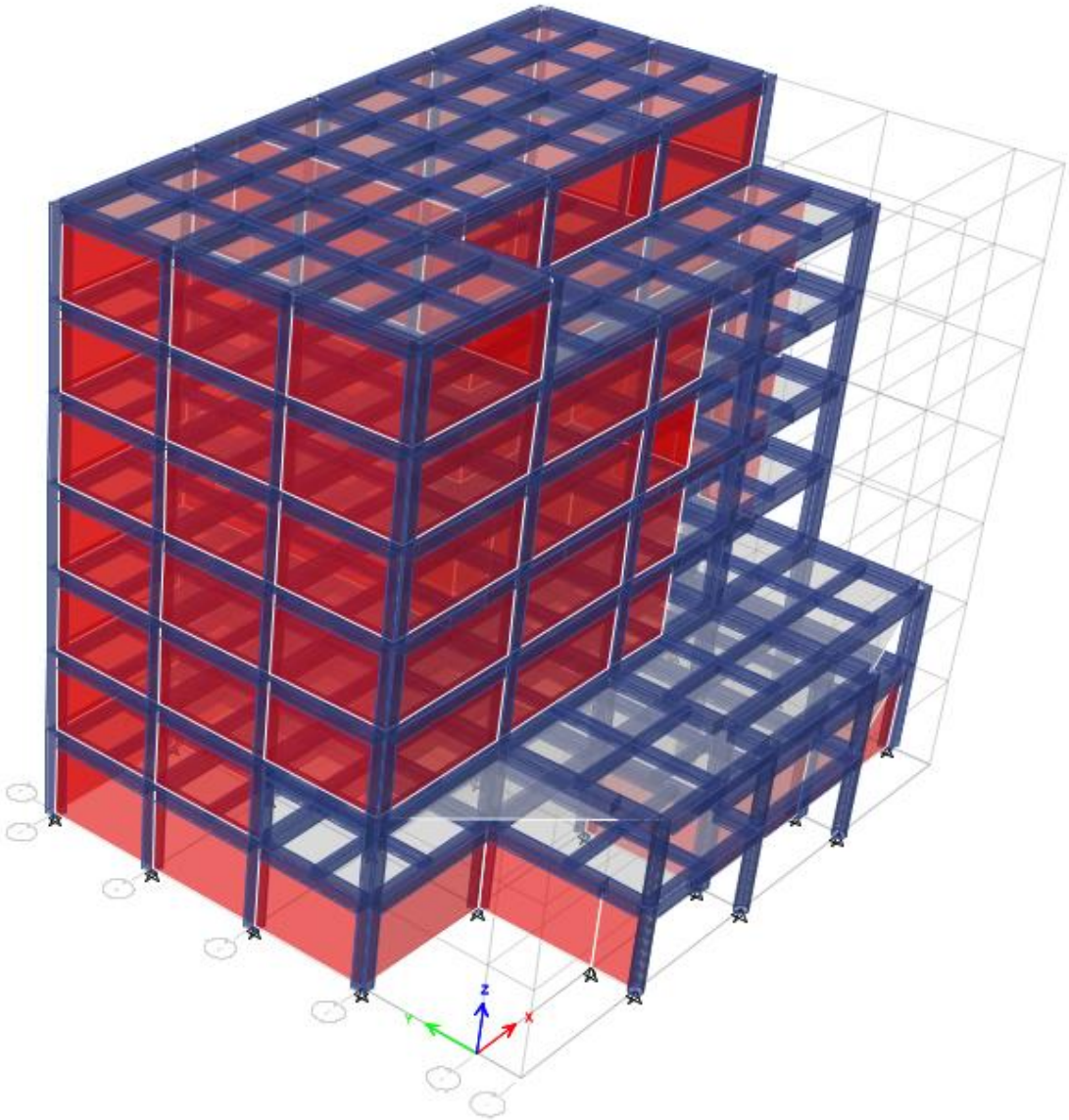

Figure B.1 :- ETABS Model for Block A

Table B.1 :- Column load Calculation of Block A

Column	Label	Output Case	Case Type	FX	FY	FZ
A3	1	Dead	LinStatic	11.8735	33.4347	2771.067
	1	Live	LinStatic	8.9007	-6.1309	708.1867
A4	2	Dead	LinStatic	11.2597	-182.293	2557.256
	2	Live	LinStatic	8.561	-77.2329	479.6572
B4	3	Dead	LinStatic	0.0832	-2.4928	1508.347
	3	Live	LinStatic	-0.2486	-1.0618	569.1462
B3	4	Dead	LinStatic	0.2196	-0.334	1879.479
	4	Live	LinStatic	-0.243	-0.2244	746.9126
C4	5	Dead	LinStatic	0.0301	-2.9227	1585.447
	5	Live	LinStatic	-0.0704	-1.2545	599.5944
C3	6	Dead	LinStatic	-0.1854	-1.5505	2023.26
	6	Live	LinStatic	-0.229	-0.8942	790.883
D4	7	Dead	LinStatic	0.7454	-2.9869	1655.093
	7	Live	LinStatic	0.486	-1.2828	618.4715
D3	8	Dead	LinStatic	0.783	-1.5829	2150.346
	8	Live	LinStatic	0.4215	-1.5663	868.2648
E4	9	Dead	LinStatic	-9.7557	-2.5682	1720.496
	9	Live	LinStatic	-7.9112	-1.0823	520.1207
E3	10	Dead	LinStatic	-10.3715	-0.1961	2340.173
	10	Live	LinStatic	-8.5708	-0.4041	788.1125
A2	11	Dead	LinStatic	145.8657	211.47	2742.737
	11	Live	LinStatic	58.8119	62.9357	811.7408
B2	12	Dead	LinStatic	-138.378	-6.3254	3092.252
	12	Live	LinStatic	-40.0178	-2.3834	1167.098
C2	13	Dead	LinStatic	-0.5136	-39.3331	2814.216
	13	Live	LinStatic	-0.5083	-18.4941	1337.569
D2	14	Dead	LinStatic	0.5299	0.9658	1631.778
	14	Live	LinStatic	-0.1344	0.1937	1437.606
E2	15	Dead	LinStatic	-9.8807	0.1195	1411.185
	15	Live	LinStatic	-8.4205	-0.0319	563.1193
B1	17	Dead	LinStatic	3.1257	71.4378	621.3293
	17	Live	LinStatic	2.7852	24.6415	231.8036
C1	18	Dead	LinStatic	26.5499	266.4118	902.7387
	18	Live	LinStatic	16.0084	134.5629	392.7941
D1	19	Dead	LinStatic	-43.7532	4.0087	711.4688
	19	Live	LinStatic	-25.7861	4.4001	295.8411
E1	20	Dead	LinStatic	-101.626	4.4055	444.1458
	20	Live	LinStatic	-56.3556	2.8438	145.4702
A5	21	Dead	LinStatic	264.272	-231.405	2345.045

Column	Label	Output Case	Case Type	FX	FY	FZ
	21	Live	LinStatic	63.3173	-55.9951	188.8063
B5	22	Dead	LinStatic	235.2427	-10.2435	2997.963
	22	Live	LinStatic	80.0344	-7.325	409.1457
C5	23	Dead	LinStatic	8.3424	-10.8506	3489.212
	23	Live	LinStatic	9.4617	-7.7807	627.3683
D5	24	Dead	LinStatic	-126.287	-10.5326	3804.027
	24	Live	LinStatic	-34.4804	-7.5241	757.0192
E5	25	Dead	LinStatic	-270.309	-6.0214	2645.34
	25	Live	LinStatic	-67.7757	-3.9313	562.9394
Bi	16	Dead	LinStatic	5.7727	-76.9929	-51.5258
	16	Live	LinStatic	4.2766	-34.0378	-32.2496
Ci	45	Dead	LinStatic	-1.7779	-2.2513	174.0009
	45	Live	LinStatic	-1.6248	-0.4696	38.0409
Di	80	Dead	LinStatic	-1.8578	-1.3704	108.4896
	80	Live	LinStatic	-0.6879	-0.4706	4.3504

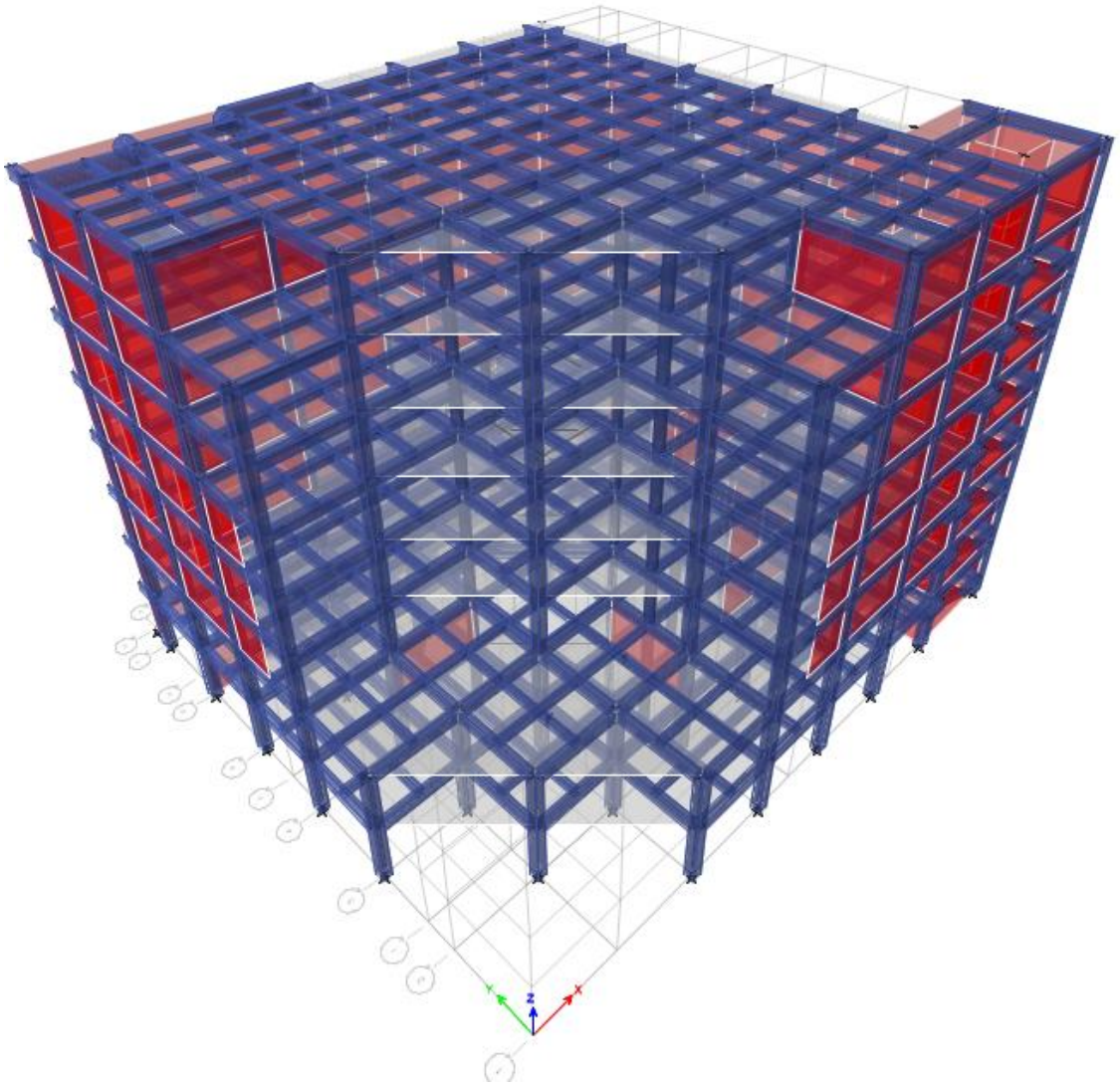

Figure B.2 :- ETABS Model for Block B

Table B.2 :- Column load Calculation of Block B

Column	Label	Output Case	Case Type	FX	FY	FZ
A7	1	Dead	LinStatic	3.3147	170.2467	1730.951
	1	Live	LinStatic	0.8922	29.8557	323.6352
B7	2	Dead	LinStatic	1.5461	-271.236	2915.064
	2	Live	LinStatic	1.977	-100.755	562.5699
A6	3	Dead	LinStatic	306.8156	-1.885	3040.029
	3	Live	LinStatic	70.645	-1.0554	660.6434
B6	4	Dead	LinStatic	136.6858	61.3963	5577.232
	4	Live	LinStatic	28.6533	-14.5223	1189.887
B5	5	Dead	LinStatic	-0.69	-2.3333	1939.235
	5	Live	LinStatic	-0.9384	-0.6362	541.6568
C6	6	Dead	LinStatic	-84.7133	72.8525	4129.756
	6	Live	LinStatic	-20.5864	4.4644	888.7057
C7	7	Dead	LinStatic	242.3134	-273.541	4192.257
	7	Live	LinStatic	56.9232	-78.5949	785.7795
D7	8	Dead	LinStatic	83.5358	95.6593	3511.216
	8	Live	LinStatic	38.7874	3.8808	588.602
D6	9	Dead	LinStatic	2.3276	-4.6229	1525.975
	9	Live	LinStatic	0.9298	-2.4282	442.248
E6	10	Dead	LinStatic	-0.869	-4.9302	1896.797
	10	Live	LinStatic	-0.3913	-1.6212	695.3861
E7	11	Dead	LinStatic	14.2845	-8.6174	2735.702
	11	Live	LinStatic	22.2083	-5.2232	499.1949
F7	12	Dead	LinStatic	9.5665	-8.8231	2448.609
	12	Live	LinStatic	9.311	-5.1998	446.6063
F6	13	Dead	LinStatic	-2.0159	-2.0567	1741.041
	13	Live	LinStatic	-0.4662	-0.2815	622.8983
G7	14	Dead	LinStatic	-114.563	-171.535	2486.542
	14	Live	LinStatic	-20.4627	-42.8111	444.2428
G6	15	Dead	LinStatic	-10.1252	-139.965	2771.037
	15	Live	LinStatic	-5.7503	-41.8916	563.25
G5	16	Dead	LinStatic	-8.4732	-59.0767	3880.495
	16	Live	LinStatic	-5.1179	-12.2395	850.2194
F5	17	Dead	LinStatic	-4.2879	-1.1257	1881.887
	17	Live	LinStatic	-1.4497	-0.5195	526.3915
F4	18	Dead	LinStatic	-3.9127	1.4612	1857.743
	18	Live	LinStatic	-2.0535	0.3973	606.2965
G4	19	Dead	LinStatic	-6.4974	269.7977	3190.017
	19	Live	LinStatic	-4.074	64.1291	711.9315
F3	20	Dead	LinStatic	-2.5243	1.7986	2155.479

Column	Label	Output Case	Case Type	FX	FY	FZ
	20	Live	LinStatic	-1.1316	0.9773	665.1287
G3	21	Dead	LinStatic	-156.291	-132.068	3082.894
	21	Live	LinStatic	-54.8412	-20.5601	628.8906
F2	22	Dead	LinStatic	-0.8075	-0.0397	1940.02
	22	Live	LinStatic	-0.3134	-0.1434	531.6537
G2	23	Dead	LinStatic	-5.3404	-120.134	2603.412
	23	Live	LinStatic	-2.5364	-14.8179	515.5458
G1	24	Dead	LinStatic	101.3786	327.4425	5120.032
	24	Live	LinStatic	7.4455	78.642	1013.12
F1	25	Dead	LinStatic	-0.6982	6.839	1901.085
	25	Live	LinStatic	-0.2585	3.9402	441.0717
A5	26	Dead	LinStatic	6.5936	-0.2384	2441.604
	26	Live	LinStatic	3.9848	-0.1667	573.1371
C5	27	Dead	LinStatic	4.0553	-1.9358	1784.926
	27	Live	LinStatic	2.7943	-0.9492	546.9289
B4	28	Dead	LinStatic	3.2651	1.9156	2382.899
	28	Live	LinStatic	0.7781	0.0468	769.9489
A4	29	Dead	LinStatic	9.6193	1.2467	1357.288
	29	Live	LinStatic	4.8683	0.3059	351.2664
C4	30	Dead	LinStatic	3.7712	-3.2451	2535.738
	30	Live	LinStatic	1.1159	0.2951	792.3928
C3	33	Dead	LinStatic	10.4491	9.2025	1963.334
	33	Live	LinStatic	2.0127	1.4227	628.0224
D2	37	Dead	LinStatic	2.5306	7.437	2673.815
	37	Live	LinStatic	0.3595	2.1155	792.0555
D3	38	Dead	LinStatic	-2.3762	1.1422	2880.553
	38	Live	LinStatic	0.5713	0.3297	843.1513
D1	39	Dead	LinStatic	1.8014	9.3349	1330.477
	39	Live	LinStatic	0.4678	4.6679	350.4741
E1	40	Dead	LinStatic	1.6507	7.7534	2268.998
	40	Live	LinStatic	0.398	4.3614	554.1544
E2	41	Dead	LinStatic	0.5848	0.2862	2392.223
	41	Live	LinStatic	0.1813	-0.2487	689.661
E3	42	Dead	LinStatic	-0.6759	3.7782	2410.159
	42	Live	LinStatic	-0.5898	2.4564	779.403
H1	43	Dead	LinStatic	-259.561	295.4396	3884.386
	43	Live	LinStatic	-61.6917	67.3982	668.1412
H2	44	Dead	LinStatic	-1.8554	140.6423	2042.114
	44	Live	LinStatic	-0.6819	68.205	268.8587
H3	45	Dead	LinStatic	-362.775	-15.2627	1436.713
	45	Live	LinStatic	-92.9285	25.5941	199.5221

Column	Label	Output Case	Case Type	FX	FY	FZ
A3	31	Dead	LinStatic	6.8865	3.953	291.5232
	31	Live	LinStatic	3.8665	1.32	101.8105
B3	32	Dead	LinStatic	1.4456	2.6001	714.3948
	32	Live	LinStatic	0.1835	0.5369	310.0206
B2	34	Dead	LinStatic	4.9434	4.5692	322.9116
	34	Live	LinStatic	2.63	2.6519	138.6461
C2	35	Dead	LinStatic	3.7818	1.4125	721.4159
	35	Live	LinStatic	1.034	0.5203	278.6785
C1	36	Dead	LinStatic	4.6554	6.5039	291.2202
	36	Live	LinStatic	1.5965	3.5975	102.8898
ai	46	Dead	LinStatic	12.8283	11.9698	1964.554
	46	Live	LinStatic	-2.2768	-2.4005	614.0713
Aiv	64	Dead	LinStatic	348.5564	-274.496	2871.003
	64	Live	LinStatic	79.0031	-56.1653	566.2223
Biv	65	Dead	LinStatic	176.653	-316.12	4141.532
	65	Live	LinStatic	57.1435	-74.2764	795.8221
Civ	66	Dead	LinStatic	79.6027	-264.875	3436.971
	66	Live	LinStatic	38.1146	-56.0759	600.0405
Div	67	Dead	LinStatic	-117.79	-191.634	1761.661
	67	Live	LinStatic	-4.1465	-39.1821	287.4883
Hst	55	Dead	LinStatic	-17.151	-69.3687	53.2201
	55	Live	LinStatic	-3.3204	-13.1126	12.8588
2	63	Dead	LinStatic	52.0592	199.9674	1466.389
	63	Live	LinStatic	2.9212	43.0242	272.8094
1	72	Dead	LinStatic	67.1465	-30.4471	1022.375
	72	Live	LinStatic	3.3402	-0.4478	146.777
4	73	Dead	LinStatic	-104.357	-52.6021	969.7214
	73	Live	LinStatic	-18.8838	-4.4879	147.0638
Hi	85	Dead	LinStatic	-266.414	0.0214	1482.307
	85	Live	LinStatic	-72.3251	0.0817	281.5642
Gi	86	Dead	LinStatic	12.0193	324.9062	2781.455
	86	Live	LinStatic	-20.4011	78.1764	565.1304
3	58	Dead	LinStatic	-203.646	178.6783	1435.526
	58	Live	LinStatic	-46.9373	34.763	276.1963
Cst	54	Dead	LinStatic	-17.5331	88.7039	53.789
	54	Live	LinStatic	-8.2839	25.037	21.0246
Stiii	79	Dead	LinStatic	39.2761	113.2563	104.7765
	79	Live	LinStatic	7.7005	37.6199	40.3266

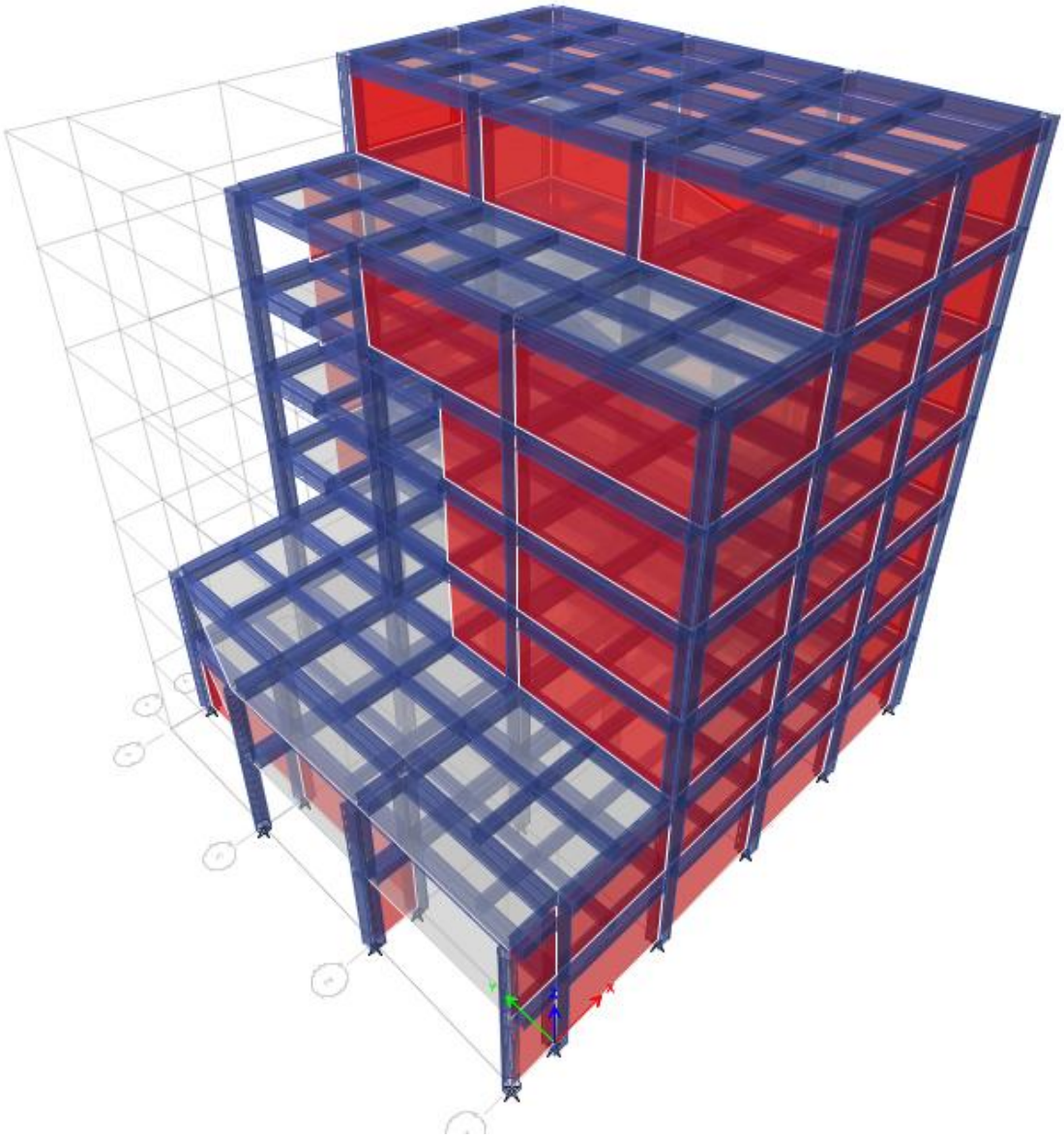

Figure B.3 :- ETABS Model for Block C

Table B.3 :- Column load Calculation of Block C

Column	Label	Output Case	Case Type	FX	FY	FZ
A4	1	Dead	LinStatic	6.1714	-41.9201	380.3016
	1	Live	LinStatic	3.1803	-22.2873	111.0002
B4	2	Dead	LinStatic	1.8856	-10.1786	1259.445
	2	Live	LinStatic	0.6932	-7.2103	426.61
B3	3	Dead	LinStatic	2.8112	0.0142	2398.1677
	3	Live	LinStatic	1.4162	0.2789	593.8393
A3	4	Dead	LinStatic	7.0953	-20.2937	795.8612
	4	Live	LinStatic	3.5027	-10.3862	303.2078
B2	5	Dead	LinStatic	2.7798	-0.6219	2375.7146
	5	Live	LinStatic	1.4476	-0.3713	587.6054
A2	6	Dead	LinStatic	-2.8989	35.8878	661.9283
	6	Live	LinStatic	0.2888	18.572	274.9352
A1	7	Dead	LinStatic	317.1043	6.9993	1063.7186
	7	Live	LinStatic	86.3422	6.2795	273.5162
B1	8	Dead	LinStatic	205.9513	10.8476	2714.2802
	8	Live	LinStatic	56.2093	8.9588	703.5592
C1	9	Dead	LinStatic	-158.8555	11.317	2737.6023
	9	Live	LinStatic	-42.0027	9.0317	706.4702
C2	10	Dead	LinStatic	-1.6905	0.3662	1973.5584
	10	Live	LinStatic	-0.2352	0.0672	917.405
C3	11	Dead	LinStatic	-0.8518	0.8713	2046.4344
	11	Live	LinStatic	0.1934	0.5694	917.5202
C4	12	Dead	LinStatic	1.2537	-9.8312	1942.2516
	12	Live	LinStatic	0.2788	-7.7444	659.2208
D4	13	Dead	LinStatic	-0.0251	-8.9921	1687.1
	13	Live	LinStatic	-0.1903	-7.4525	505.6429
D3	14	Dead	LinStatic	-1.1135	1.2902	1669.015
	14	Live	LinStatic	-0.6241	0.6442	937.3224
E4	15	Dead	LinStatic	-3.153	-223.1591	3116.3119
	15	Live	LinStatic	-3.319	-57.2608	670.489
E3	16	Dead	LinStatic	-8.3115	27.4351	3806.1543
	16	Live	LinStatic	-7.6034	-1.4267	835.3107
D2	17	Dead	LinStatic	-1.4096	0.4044	1049.58
	17	Live	LinStatic	-0.6832	0.1672	565.461
D1	18	Dead	LinStatic	-303.8141	10.4247	2000.5079
	18	Live	LinStatic	-86.7781	8.2579	491.0602
E1	19	Dead	LinStatic	-222.2075	118.9546	1688.8257
	19	Live	LinStatic	-62.7502	34.558	360.1251
E2	20	Dead	LinStatic	-8.2115	90.3889	2552.5348

Column	Label	Output Case	Case Type	FX	FY	FZ
	20	Live	LinStatic	-7.1167	26.021	562.1438
a3	21	Dead	LinStatic	-0.0904	-0.0583	35.9421
	21	Live	LinStatic	-0.0987	-0.1175	10.4362
a2	22	Dead	LinStatic	46.3912	-0.3434	161.5166
	22	Live	LinStatic	24.1248	-0.1083	67.0692
a1	23	Dead	LinStatic	121.1892	0.197	355.4217
	23	Live	LinStatic	33.7243	0.9595	92.9594

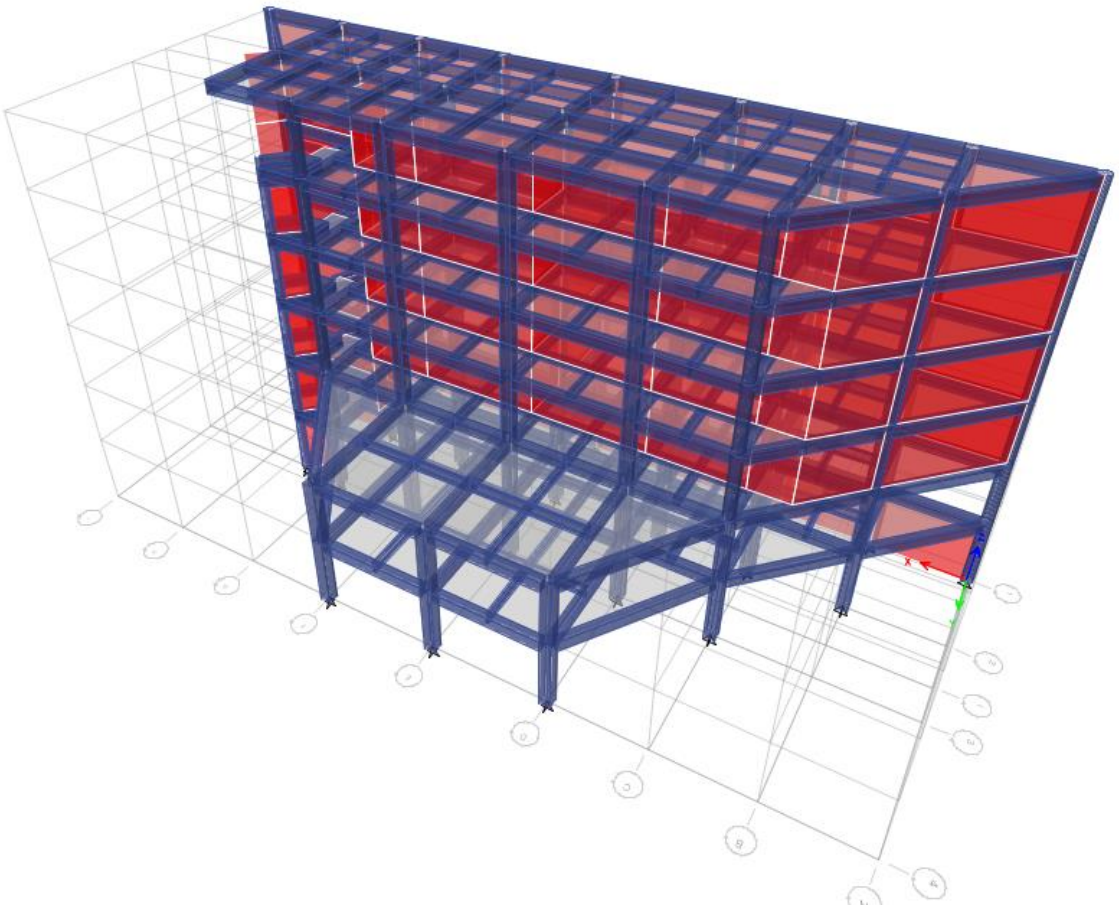

Figure B.4 :- ETABS Model for Block D

Table B.4 :- Column load Calculation of Block D

Column	Label	Output Case	Case Type	FX	FY	FZ
A1	3	Dead	LinStatic	128.2671	7.3972	1421.848
	3	Live	LinStatic	24.1424	2.1003	167.8961
B1	4	Dead	LinStatic	37.6448	14.5027	1903.805
	4	Live	LinStatic	19.0501	5.1682	284.7659
B2	5	Dead	LinStatic	1.0997	1.8648	2485.117
	5	Live	LinStatic	1.8566	-1.8514	294.1952
C3	7	Dead	LinStatic	3.2507	3.0432	2217.48
	7	Live	LinStatic	2.4524	-1.0971	237.0296
C2	8	Dead	LinStatic	-0.6026	2.527	1789.964
	8	Live	LinStatic	-0.0032	-0.104	407.7122
C1	9	Dead	LinStatic	70.3154	13.0127	1731.073
	9	Live	LinStatic	16.3422	5.4436	323.1338
D1	10	Dead	LinStatic	68.1011	13.991	1819.069
	10	Live	LinStatic	15.8515	6.2543	376.1613
D2	11	Dead	LinStatic	2.2295	2.4135	1873.114
	11	Live	LinStatic	1.0374	0.0742	448.2675
D3	12	Dead	LinStatic	2.8498	5.8083	2069.88
	12	Live	LinStatic	1.9541	2.5194	384.3262
E3	13	Dead	LinStatic	0.1232	6.0832	2144.173
	13	Live	LinStatic	-0.0813	4.1	453.7499
E2	14	Dead	LinStatic	-0.4331	2.5305	2310.106
	14	Live	LinStatic	-0.1084	-0.1262	410.9755
E1	15	Dead	LinStatic	67.6111	16.3166	1895.415
	15	Live	LinStatic	13.4016	7.4697	414.8129
F3	16	Dead	LinStatic	-0.8027	4.175	1878.884
	16	Live	LinStatic	-2.3102	2.8003	379.6105
F2	17	Dead	LinStatic	-0.2291	3.0421	1658.896
	17	Live	LinStatic	-1.9132	0.0376	397.3637
F1	18	Dead	LinStatic	40.0317	13.6157	1600.964
	18	Live	LinStatic	6.5585	6.2416	364.2248
G1	19	Dead	LinStatic	10.5192	11.6002	1305.945
	19	Live	LinStatic	2.0748	5.043	303.0285
G2	20	Dead	LinStatic	83.9901	5.1205	3965.661
	20	Live	LinStatic	5.3513	-0.3545	638.2374
G3	21	Dead	LinStatic	2.5412	-1.3861	2374.107
	21	Live	LinStatic	-1.0984	0.2105	288.5471
H2	23	Dead	LinStatic	-506.376	238.2542	4000.867
	23	Live	LinStatic	-99.5335	36.5677	640.527
H1	24	Dead	LinStatic	-25.4526	10.891	1073.827

Column	Label	Output Case	Case Type	FX	FY	FZ
	24	Live	LinStatic	-4.6954	4.4739	257.8009
I1	27	Dead	LinStatic	-53.4337	8.2641	561.8117
	27	Live	LinStatic	-15.3654	2.2242	138.883
E5	28	Dead	LinStatic	0.6036	-10.7146	521.0327
	28	Live	LinStatic	-0.1315	-8.7588	229.7124
D5	29	Dead	LinStatic	2.2336	-11.0335	443.4707
	29	Live	LinStatic	2.0822	-7.028	157.2888
F5	30	Dead	LinStatic	-2.2153	-10.4338	438.9199
	30	Live	LinStatic	-2.3774	-7.0329	156.7745
St3	44	Dead	LinStatic	90.3545	-232.965	174.8351
	44	Live	LinStatic	16.9854	-40.1021	34.0774
sta	45	Dead	LinStatic	38.7036	-69.1589	80.741
	45	Live	LinStatic	10.7311	-14.4302	19.7289
stb	85	Dead	LinStatic	-60.9253	-48.7613	567.1876
	85	Live	LinStatic	-12.2535	-9.8433	88.7004

APPENDIX - C COEFFICIENT OF CONSOLIDATION

The coefficient of consolidation, Cv, can be determined from square root of time method. Data for curve were taken from soil report of *CMTL (2002)*. The curve was plotted between the dial gauge reading and square root of time. Coefficient of consolidation can be determined from the different curve plotted on every incremental load and taking the average value.

Calculation of C_v of BH1

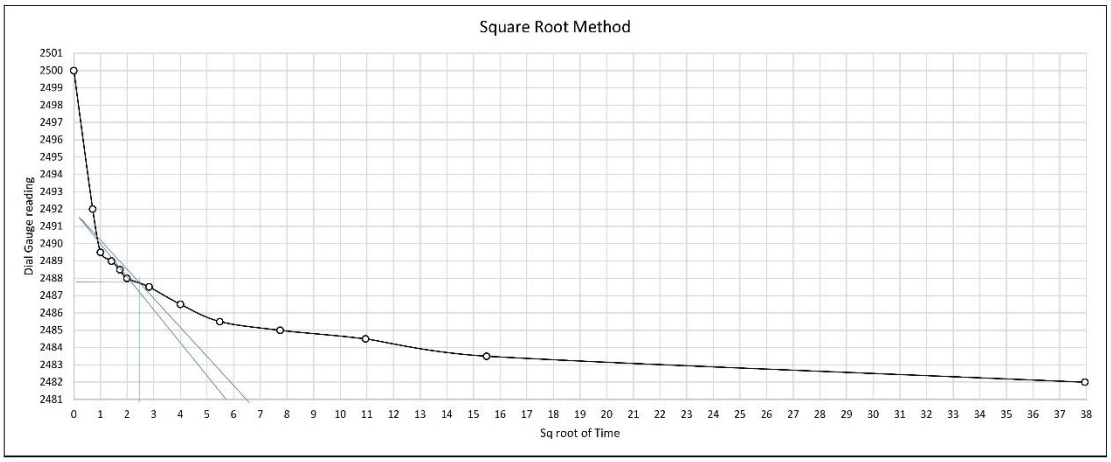

Figure C.5 :- Chart of Square Root Method

For Pressure 0.3 t/m²

Calculation of Cv

d_0 = 2491.5

sq root of t_0 = 5.5

As per Tayler's Method, sq root of t_0 is increased by 15% to determine d_{90}

So, sq root t_0 = 6.325

d_{90} = 2487.8

Now,

$$d_{100} = d_o - \frac{10}{9}(d_0 - d_{9o})$$

d_{100} = 2487.389

And,

$$d_{50} = \frac{1}{2}(d_0 - d_{9o})$$

d_{50} = 2489.444

sq root t_{50} 0.9

t_{50} = 0.81

H_i = 20 mm

H_f = 19.894 mm

D_{50} = 9.974 mm

Then we get C_{v1} by,

$$C_{v1} = \frac{T_{50} * H_{50}^2}{t_{50}}$$

C_{v1} = 2.4193*10^{-5} m^2/min

Similarly,

C_{v2} = 2.38*10^{-5} m^2/min

C_{v3} = 2.35*10^{-5} m^2/min

C_{v4} = 2.31*10^{-5} m^2/min

C_{v5} = 2.25*10^{-5} m^2/min

C_{v6} = 2.18*10^{-5} m^2/min

C_{v7} = 2.09*10^{-5} m^2/min

C_{v8} = 1.99*10^{-5} m^2/min

Average value of coefficient of Consolidation ($C_{v\ avg}$) = 2.26*10^{-5} m^2/min

$C_{v\ avg}$ = 0.0323 m^2/day

Determination of Degree of Consolidation before construction of Block D

t = 2953 days

$$T_v = \frac{c_v * t}{d^2}$$

T_v = 0.663

Now,

Tv = -0.933 $\log_{10}$ (1-U) – 0.085 (for U > 0.60)

U = 0.8423 = 84.23%

Determination of Degree of Consolidation after construction of Block D (present)

t = 6740 days

$$T_v = \frac{c_v * t}{d^2}$$

$T_v = 1.514$

Now,

$T_v = -0.933 \log_{10}(1-U) - 0.085$ (for U > 0.60)

U = 0.9807 = 98.07%

Similarly, the process was repeated for all the bore hole data and the data re summarized below,

Table C.1:- Summary of Coefficient of Consolidation and Degree of Consolidation of all Borehole

S.N.	Borehole Log	C_v (m^2/day)	Before Block D construction		Present Time	
			T_v	U (%)	T_v	U (%)
1	BH 1	0.0323	0.663	84.23	1.514	98.07
2	BH 2	0.0310	0.637	83.156	1.453	97.75
3	BH 3	0.0318	0.651	83.76	1.487	97.93
4	BH 4	0.0323	0.565	79.904	1.290	96.641
5	BH 5	0.0319	0.777	88.096	1.774	98.983
Average		**0.032**	**0.659**	**83.829**	**1.504**	**97.875**

For Settlement of building,

Degree of Consolidation (U) = 97.875%

We have,

$$U = \frac{S_t}{S_f}$$

From Terzaghi,

S_t = 183.19 mm

Therefore, S_f = 179.297 mm

Settlement of building is currently as per Terzaghi 179.297 mm.

From Janbu,

S_t = 176.071 mm

Therefore, S_f = 172.329 mm

Settlement of building is currently as per Janbu 172.329 mm.